Title: Mapping adolescent reward anticipation, receipt and prediction error during the Monetary Incentive Delay task

Zhipeng Cao[1,2]; Marc Bennett Ph.D.[2]; Catherine Orr Ph.D.[3]; Ilknur Icke Ph.D.[3], Tobias Banaschewski M.D., Ph.D.[4]; Gareth J Barker Ph.D.[5]; Arun L.W. Bokde Ph.D.[6]; Uli Bromberg Ph.D.[7]; Christian Büchel M.D.[7]; Erin Burke Quinlan, Ph.D.[8]; Sylvane Desrivières Ph.D.[8]; Herta Flor Ph.D.[9,10]; Vincent Frouin Ph.D.[11]; Hugh Garavan Ph.D.[3]; Penny Gowland Ph.D.[12]; Andreas Heinz M.D., Ph.D.[13]; Bernd Ittermann Ph.D.[14]; Jean-Luc Martinot M.D., Ph.D.[15] Frauke Nees Ph.D.[4,9]; Dimitri Papadopoulos Orfanos Ph.D.[11]; Tomáš Paus M.D., Ph.D.[16]; Luise Poustka M.D.[17,18]; Sarah Hohmann M.D.[4]; Juliane H. Fröhner M.Sc[19]; Michael N. Smolka M.D.[19]; Henrik Walter M.D., Ph.D.[13]; Gunter Schumann M.D.[8]; Robert Whelan Ph.D.[2,20]; IMAGEN Consortium

[1]School of Psychology, University College Dublin, Ireland;
[2]School of Psychology and Institute of Neuroscience, Trinity College Dublin, Dublin 2, Ireland;
[3]Departments of Psychiatry and Psychology, University of Vermont, 05405 Burlington, Vermont, USA;

[4]Department of Child and Adolescent Psychiatry and Psychotherapy, Central Institute of Mental Health, Medical Faculty Mannheim, Heidelberg University, Square J5, 68159 Mannheim, Germany;

[5]Centre for Neuroimaging Sciences, Institute of Psychiatry, Psychology & Neuroscience, King's College London, United Kingdom;

[6]Discipline of Psychiatry, School of Medicine and Trinity College Institute of Neuroscience, Trinity College Dublin, Dublin, Ireland;

[7]University Medical Centre Hamburg-Eppendorf, House W34, 3.OG, Martinistr. 52, 20246, Hamburg, Germany;

[8]Centre for Population Neuroscience and Stratified Medicine (PONS) and MRC-SGDP Centre, Institute of Psychiatry, Psychology & Neuroscience, King's College London, United Kingdom;

[9]Department of Cognitive and Clinical Neuroscience, Central Institute of Mental Health, Medical Faculty Mannheim, Heidelberg University, Square J5, Mannheim, Germany;

[10]Department of Psychology, School of Social Sciences, University of Mannheim, 68131 Mannheim, Germany;

[11]NeuroSpin, CEA, Université Paris-Saclay, F-91191 Gif-sur-Yvette, France;

[12]Sir Peter Mansfield Imaging Centre, School of Physics and Astronomy, University of Nottingham, University Park, Nottingham, United Kingdom;

[13]Department of Psychiatry and Psychotherapy, Campus Charité Mitte, Charité, Universitätsmedizin Berlin, Charitéplatz 1, Berlin, Germany;

[14]Physikalisch-Technische Bundesanstalt (PTB), Braunschweig and Berlin, Germany

[15]Institut National de la Santé et de la Recherche Médicale, INSERM Unit 1000 "Neuroimaging & Psychiatry", University Paris Sud – Paris Saclay, University Paris Descartes; Service Hospitalier Frédéric Joliot, Orsay; and Maison de Solenn, Paris, France

[16]Rotman Research Institute, Baycrest and Departments of Psychology and Psychiatry, University of Toronto, Toronto, Ontario, M6A 2E1, Canada;

[17]Department of Child and Adolescent Psychiatry and Psychotherapy, University Medical Centre Göttingen, von-Siebold-Str. 5, 37075, Göttingen, Germany;

[18]Clinic for Child and Adolescent Psychiatry, Medical University of Vienna, Währinger Gürtel 18-20, 1090, Vienna, Austria;

[19]Department of Psychiatry and Neuroimaging Center, Technische Universität Dresden, Dresden, Germany;

[20]Global Brain Health Institute, Trinity College Dublin, Ireland;

Correspondence to Dr. Robert Whelan, School of Psychology, Trinity College Dublin, Dublin 2, Ireland. E-mail: robert.whelan@tcd.ie

Running title: Mapping the adolescent reward system

Keywords: adolescence; reward processing; functional connectivity; gender differences; sensation seeking

Abstract

The functional neuroanatomy and connectivity of reward processing in adults are well documented, with relatively less research on adolescents, a notable gap given this developmental period's association with altered reward sensitivity. Here, a large sample (n = 1,510) of adolescents performed the monetary incentive delay (MID) task during functional magnetic resonance imaging. Probabilistic maps identified brain regions that were reliably responsive to reward anticipation and receipt, and to prediction errors derived from a computational model. Psychophysiological interactions analyses were used to examine functional connections throughout reward processing. Bilateral ventral striatum, pallidum, insula, thalamus, hippocampus, cingulate cortex, midbrain, motor area and occipital areas were reliably activated during reward anticipation. Bilateral ventromedial prefrontal cortex and bilateral thalamus exhibited positive and negative activation, respectively, during reward receipt. Bilateral ventral striatum was reliably active following prediction errors. Previously, individual differences in the personality trait of sensation seeking were shown to be related to individual differences in sensitivity to reward outcome. Here, we found that sensation seeking scores were negatively correlated with right inferior frontal gyrus activity following reward prediction errors estimated using a computational model. Psychophysiological interactions demonstrated widespread cortical and subcortical connectivity during reward processing, including connectivity between reward-related regions with motor areas and the salience network. Males had more activation in left putamen, right precuneus and middle temporal gyrus during reward anticipation. In summary, we

found that, in adolescents, different reward processing stages during the MID task were robustly associated with distinctive patterns of activation and of connectivity.

The capacity to anticipate and detect rewarding outcomes is fundamental for the development of goal-orientated behavior and efficient decision-making. Alterations in reward sensitivity during adolescence contribute to the emergence of impulsive decisions and risk-taking behaviors, such as substance-use (Jollans, et al., 2016; Karoly, et al., 2015; Weiland, et al., 2013). Reward system dysfunction is also involved in the pathogenesis of numerous psychiatric disorders during adolescence, such as ADHD (Ma, et al., 2016; Scheres, et al., 2007). Given that adolescence is a neurodevelopmental period associated with an altered sensitivity to rewarding outcomes and situations, mapping the neural correlates of different stages of reward processing in adolescence is important.

Reward processing involves discrete anticipation and outcome stages that each recruit overlapping and distinct brain regions. These stages and their neural correlates can be effectively isolated using the monetary incentive delay (MID) task with concurrent functional magnetic resonance imaging (fMRI) (Knutson, et al., 2000). In this task, an incentive cue signals a likely reward (e.g., 10 c) or non-reward (i.e., 0 c) and then a target stimulus prompts a speeded behavioral response (e.g., a button-press in response to a blue square**).** Simple feedback then denotes the receipt or, alternatively the infrequent omission, of the reward. In adolescents, the reward anticipation period is associated with increased activation in the ventral striatum (VS), insula, thalamus, caudate and supplemental motor area (SMA); additionally, VS activity is positively associated with the amount of the likely reward (Bjork, et al., 2004; Bjork, et al., 2010). A review of 26 studies (Silverman, et al., 2015) that used a variety of differing reward-related tasks (e.g., delay discounting tasks, MID tasks) indicated that, during

adolescence, reward anticipation activates left nucleus accumbens (NAcc), right caudate, right insula, left frontal operculum cortex and left supplementary motor cortex.

Reward receipt is associated with increased activation in the ventromedial prefrontal cortex (vmPFC) in adolescents (Bjork, et al., 2004; Bjork, et al., 2010). A wealth of evidence from adult studies suggests that vmPFC activation is associated with reward valuation (Levy and Glimcher, 2011; Peters and Büchel, 2010; Smith, et al., 2010) and magnitude (Diekhof, et al., 2012). The VS is also active when there is a mismatch between the expected and actual reward outcome (i.e., a prediction error; PE) (Hare, et al., 2008; Peters and Buchel, 2010). VS activity increases when the actual reward is greater than what was predicted (i.e., positive PE), (ii) decreases when the actual reward is less than what was anticipated (i.e., negative PE) and (iii) remains static when there is no discrepancy between what is expected and what is received (Schultz, 2016). Reward PEs can be detected by contrasting brain activity from trials in which expected rewards were delivered against trials in which rewards were unexpectedly omitted. Furthermore, computational modeling (e.g., using a Rescorla-Wagner model; Rescorla and Wagner, 1972) of the task-based signal-reward contingencies can be used to estimate each individual's trial-by-trial prediction errors (Glascher and O'Doherty, 2010). The specificity of the vmPFC and VS for reward receipt and PE, respectively, has been shown previously in adults (Rohe, et al., 2012).

The different stages of reward processing are characterized by distinct changes in functional connectivity among different brain regions. For example, Silverman et al. (2015) proposed that, during reward receipt in adolescents, projections from insula and orbitofrontal cortex (OFC) allow the integration of reward evaluation and incentive-based behavioral activation in VS. From the

perspective of adolescent development, interactions between brain regions such as VS and regions in the prefrontal cortex (PFC) are emphasized in neurobiological models such as the dual-system model, the triadic model and the imbalance model (see Casey, 2015 for a review). Functional connectivity between brain regions can be quantified using a psychophysiological interactions (PPI) analysis (Friston, et al., 1997), which examines if correlation in activity between seed regions and the rest of the brain vary as a function of the experimental manipulation. This method has been employed in previous research into adolescent reward-processing (Ernst, et al., 2015; van den Bos, et al., 2012; van den Bos, et al., 2015). PPI analyses have shown, for example, that VS-PFC connectivity predicted the updating of outcome expectancy following negative feedback during a probabilistic learning task in children, adolescent and adults (van den Bos, et al., 2012).

Biological factors such as gender and pubertal development are known to influence adolescent brain functions (Azim, et al., 2005; Blakemore, et al., 2010; Forbes, et al., 2011; Forbes, et al., 2010; Goddings, et al., 2014; Haase, et al., 2011; Klapwijk, et al., 2013; Moore, et al., 2012; Munro, et al., 2006; Urosevic, et al., 2014). For instance, longitudinal research suggests that pubertal development is significantly positively correlated with the structural volumes of amygdala and hippocampus, and negatively correlated to volumes of NAcc, caudate, putamen and globus pallidus (Goddings, et al., 2014). Furthermore, adolescents at a more advanced pubertal stage exhibited less striatal and more medial prefrontal cortex (mPFC) activation during reward processing than those at a less advanced pubertal stage (Forbes, et al., 2010). An understanding of the impact of these factors impact could shed light on gender ratios of adolescent psychiatric disorders as well as their developmental trajectories. Typically, the effects of gender and puberty have not been analysed or have been controlled for

statistically in previous reward processing studies (Bjork, et al., 2004; Bjork, et al., 2010; Jia, et al., 2016; Peters, et al., 2011; Stringaris, et al., 2015), which make their specific contribution in reward processing unclear.

Sensation seeking is a reward-related personality characteristic that involves seeking novel or intense sensations and experiences, and a willingness to take risks for the sake such experiences (Zuckerman, 2014). Sensation seeking is a predictor of risk-taking behaviour during adolescence, including intentions to try smoking and drinking (Jurk, et al., 2015; Memetovic, et al., 2016). Structural and functional VS variations were previously associated with sensation seeking in adolescents (Hawes, et al., 2017; Yang, et al., 2015). Also, a recent study demonstrated that high sensation seeking adolescents (n = 27, mean age: 14.12 years-old), compared with low sensation seeking adolescents (n = 27, mean age: 13.75 years-old), had greater bilateral insula and IFG brain responses to reward receipt versus reward absence during a Wheel of Fortune decision making task (Cservenka, et al., 2013). Differences were only apparent when comparing tertiles of high and low sensation seeking scores. Cservenka and colleagues did not find brain regions that correlated with sensation seeking nor did they find that NAcc activity correlated with sensation seeking. The latter result is consistent with another study (n = 139) that used an incentivized anti-saccade task with mid-adolescents (age range = 12-16 years old) (Hawes, et al., 2017) and reported the absence of a correlation between reward-related NAcc activity and sensation seeking.

There are a limited number of empirical investigations into adolescent reward processing and extant studies have employed small sample sizes (Bjork, et al., 2004; Bjork, et al., 2010), as is typical for functional neuroimaging studies (Button, et al., 2013). Meta-analyses of reward processing exist

(Liu et al., 2011; Silverman et al., 2016). However, these have amalgamated data from a range of different reward-related tasks with widely different methodological parameters (e.g., delay discounting, gambling tasks and MID tasks) that likely evoke different patterns of brain activity. The MID task is currently used in multisite longitudinal neuroimaging studies, such as IMAGEN (Schumann, et al., 2010), and the Adolescent Brain and Cogntive Development study (ABCD; Casey, et al., 2018). Therefore, a precise characterization of the neural correlates of the MID task would be advantageous. PPI is a useful method but – due to the inclusion of correlated regressors in the same model – has low statistical power, particularly for event-related designs (O'Reilly, et al., 2012): large sample sizes can ameliorate this drawback of PPI.

In this study, adolescents from a community-based sample and multicenter fMRI study performed the MID task (Schumann, et al., 2010). These adolescents were 14 years-old on average, a key developmental period for risk-taking behavior and for the emergence of psychiatric symptoms (Schumann, et al., 2010). We first created probabilistic maps of activation to identify regions reliably activated during reward anticipation, receipt and infrequent reward omission. Constructing probabilistic maps has proven useful for interrogating large neuroimaging datasets, including IMAGEN. For example, Tahmasebi and colleagues identified regions that were reliably activated in response to emotional faces (Tahmasebi, et al., 2012). Second, PPI analyses were conducted to investigate the functional connectivity with respect to reward anticipation, receipt and instances of infrequent reward omission. Based on prior findings (Silverman, et al., 2015), we expected to observe activation in SMA, VS, insula, and caudate during reward anticipation. In line with previous studies showing increased vmPFC activation during reward outcome (Bjork, et al., 2004; Bjork, et al., 2010),

we expected similar findings during reward receipt. For the infrequent reward omission, we predicted that the VS would be activated. Furthermore, we applied the Rescorla-Wagner reinforcement learning model to first estimate trial-by-trial reward PE and then describe its neural correlates. As reward PE is observed primarily in VS (Garrison, et al., 2013), we predicted that the modulation effects of trial-by-trial estimated reward PE to be observed in VS. For the functional connectivity, we expected to observe the involvement of a wide range brain networks such as visual, salience, sensorimotor and control networks in reward processing, which could be represented by the connections between seed regions and typical areas such as occipital lobe, motor areas, insula, SMA and frontal areas (Silverman, et al., 2015; van den Bos, et al., 2012; van den Bos, et al., 2015). To clarify the role of other biological factors, we directly compared activation and connectivity patterns between males and females, and between early and late pubertal stages. Finally, we correlated sensation seeking scores with brain activation and connectivity during reward processing to examine neural correlates of this personality trait.

MATERIALS AND METHODS

Participants

Adolescents (n = 1510, 795 females) from the IMAGEN project were included in the present study, with data collected from eight sites (France, United Kingdom, Ireland, Germany). The project was approved by all local ethics research committees, and informed consent was obtained from participants and their parents/guardians. A detailed description of the study protocol and data acquisition has been previously published (Schumann, et al., 2010).

MRI Data Acquisition

Magnetic resonance imaging (MRI) acquisition was performed with a 3T MRI system from various manufacturers (Siemens, Philips, General Electric, and Bruker). Standardized hardware for visual and auditory stimulus presentation (Nordic Neurolabs, Bergen Norway) was used at all sites. To minimize effects of different scanners, a set of acquisition parameters compatible with all scanners was used across sites. High resolution T1-weighted structural images were acquired (sagittal slice plane, repetition time = 2,300 ms, echo time = 2.8 ms, flip angle = 8°, matrix = 256×256, field of view = 280×280 mm^2) for anatomical localization and co-registration with the functional time series. Blood-oxygen-level-dependent (BOLD) images were acquired with a gradient echo-planar imaging (EPI) sequence using similar acquisition parameters across sites (i.e., oblique slice plane, repetition time = 2200 ms, echo time = 30 ms, flip angle = 75°, matrix = 64×64, field of view = 220×220 mm^2, 40 slices with 2.4-mm slice thickness and 1-mm gap; 300 volumes per run). The relatively short echo time was used to optimize imaging of subcortical areas. Two quality control procedures were implemented at each site: (1) The American College of Radiology phantom was scanned to provide information about geometric distortions and signal uniformity related to hardware differences in radiofrequency coils and gradient systems, image contrast and temporal stability and (2) several healthy volunteers were regularly scanned at each site to determine inter-site variability in structural and functional measures (for example, tissue contrast in raw MRI signal, tissue relaxation properties). Further details of MRI acquisition and quality control procedures have been described previously (Schumann, et al., 2010).

Monetary Incentive Delay Task

Participants performed a variant of the MID task, in which small and large monetary gains were indicated by different cues (see Figure 1). On each trial, an incentive cue indicating potential rewards was displayed on the left or right side of a black screen for 250 ms. There were three types of incentive cues (i.e. three within-subject conditions): a circle with two lines (large reward: 10 points), a circle with one line (small reward; 2 points) and a triangle (no reward: 0 points). Subsequently, a blank black screen was presented for 4000 to 4500 ms, followed by a target screen in which participants were asked to respond to a target stimulus by pressing a button (with left or right hand). Responding too early or too late resulted in a failure to gain the points (i.e., reward miss). Responding within the response interval resulted in gaining the points (i.e., reward hit). The response interval was adjusted to produce a 66% success rate: the response interval was shortened if the success rate exceeded 66% (making the task more difficult), and lengthened if the success rate was below 66% (making the task easier). Then, the points won in this trial as well as the accumulated points won by previous trials were displayed. The response and feedback screens lasted a total of 2000 ms. The inter-trial interval was 3500-4150 ms, during which a fixation cross was presented. There were 66 trials in total and 22 trials per condition.

[Insert Figure 1 about here]

Puberty Development

The pubertal status of adolescents was assessed using the computerized Pubertal Development Scale (PDS; Petersen, Crockett & Richards, 1988), which is an 8-item self-report assessment of physical development. Pubertal status is estimated on a 5 point-scale where 1 = prepubertal, 2 = beginning

pubertal, 3 = midpubertal, 4 = advanced pubertal, 5 = postpubertal. Psytools (Delosis, London), an online platform for self-assessment, was used to collect the pubertal measure.

Intelligence

Intelligence was assessed by a version of Wechsler Intelligence Scale for Children WISC-IV (Wechsler, 2003) with following subscales included: Perceptual Reasoning, consisting of Block Design (arranging bi-colored blocks to duplicate a printed image) and Matrix Reasoning (a series of colored matrices are presented and the adolescent is asked to select the consistent pattern from a range of options); and Verbal Comprehension, consisting of Similarities (two similar but different objects or concepts are presented and the adolescent is asked to explain how they are alike or different) and Vocabulary (a picture is presented or a word is spoken aloud by the experimenter and the adolescent is asked to provide the name of the depicted object or to define the word).

Sensation Seeking

Sensation seeking was measured with a 23-item (4-point Likert scale "1 = Strong Disagree" to "4 = Strongly Agree") subscale in the Substance Use Risk Profile Scale (SURPS; Woicik et al., 2009). The SURPS assesses personality traits that confer risk for substance misuse and psychopathology. Four distinct and independent personality dimensions; anxiety sensitivity, hopelessness, sensation seeking, and impulsivity are measured by SURPS. The SURPS is a valid instrument for measuring sensation seeking (Schlauch, et al., 2015).

fMRI preprocessing and analysis

Analyses were performed using Statistical Parametric Mapping software package (Wellcome Trust Centre for Neuroimaging, London). The preprocessing was completed using SPM8 with the subsequent

statistical analyses conducted using SPM12. Time series data were corrected for slice timing, then for movement, non-linearly warped onto Montreal Neurological Institute (MNI) space using a custom EPI template (53 × 63 × 46 voxels) created out of an average of the mean images of 400 adolescents, and Gaussian-smoothed using a 5-mm full-width half-maximum kernel. Automatic and visual (web-based) quality control procedures of pre-processed structural and functional MRI were implemented. Data were screened for normalization issues, segmentation issues, clinical abnormalities, motion artifacts, deformation, and susceptibility artifacts.

Eight conditions and 6 estimated movement parameters (3 translations, 3 rotations) were included in the individual level general linear model (GLM), which used SPM's default hemodynamic response function (HRF). The conditions were: (i) the no-reward cue, (ii) the small-reward cue, (iii) the large-reward cue, (iv) no reward (i.e. no-reward hit and miss), (v) small-reward hit, (vi) small-reward miss, (vii) large-reward hit and (viii) large-reward miss. In the group level analyses, gender, pubertal stage, handedness and 7 dummy-coded acquisition sites were added in as nuisance covariates, unless otherwise stated. For all fMRI analyses, we used SPM's voxel-wise FWE correction at $p<0.05$. For interpretability (i.e., to exclude very small clusters) we also applied a cluster extent threshold of 10 contiguous voxels for connectivity maps and gender and puberty analyses. Results with cluster extent set to 1 are displayed in Supplementary Table S2-S7.

In the following group level and connectivity analyses, we focused on 3 specific contrasts. First, *reward anticipation* was estimated as large-reward cue minus no-reward cue. Second, *reward receipt* was estimated as large-reward hit minus no reward. Third, *infrequent reward omission* was estimated as large-reward miss minus large-reward hit (i.e., the cue signaled a large reward was potentially available

but the reward was not delivered). Previous studies have revealed the impact of reward magnitude on reward-related responses, with larger reward eliciting greater activity in reward-related regions (Bjork, et al., 2010; Yacubian, et al., 2006). Thus, we focused on the large reward to attain the maximal sensitivity to detect associations with reward-relate neural response, which has been done in previous studies (Schneider, et al., 2012a; Schneider, et al., 2012b).

Probabilistic mapping. For the activation analyses, results of the group-level analyses with the whole sample of 1,510 participants were robust (a cluster with 37,258 voxels was suprathreshold for reward anticipation at a voxel-wise FWE $p < 10^{-11}$). Therefore, we adopted the probability mapping approach similar to Tahmasebi and colleagues (2011). Specifically, a random sample of 100 participants (50 males and 50 females) were selected from the whole sample and then entered into a group level analysis. Next, these t-maps were thresholded at voxel-wise FWE-corrected $p < 0.05$, and binarized (i.e., 1 for significant, 0 for non-significant). These steps were repeated **100** times with a new random sample of 100, for each iteration, which generated a set of **100** binarized t-maps that were then averaged to obtain probabilistic maps. Regions showing probability of activation above 0.8 (i.e. over 80% of samples) were reported with peak probability, MNI coordinates and corresponding *t* value from normal group level results. If the peak probability of activation was the same for two or more voxels in the same region (e.g., two voxels with a probability of 1), the MNI coordinates for the voxel having highest *t* value were reported.

Connectivity mapping. Connectivity maps of seed regions during reward anticipation, receipt and PE were obtained by PPI analyses (Friston, et al., 1997). The selection of seed regions was based on peak activity with respect to the probabilistic maps from the contrasts. If several regions showed the same

peak probability of activation (e.g., several regions with a probability of 1 during reward anticipation), the region that had highest *t* value as well as its bilateral counterpart were selected as seed regions. Thus, chosen seed regions were bilateral thalamus (left: [-9, -19, 7] and right: [9, -19, 7]) for the reward anticipation, bilateral vmPFC (left: [-3, 41, 7] and right: [3, 41, 7]) and bilateral thalamus (left: [-9, -19, 7] and right: [9, -19, 7]) for reward receipt and bilateral VS (left: [-12, 14, -8] and right: [12, 14, -8]) for infrequent reward omission. In addition, bilateral VS (left: [-12, 14, -8] and right: [12, 14, -8]) were also included as seed regions for reward anticipation given that VS has been a region of interest in previous reward processing studies (Haber and Knutson, 2010; Liu, et al., 2011; Lorenz, et al., 2014; Silverman, et al., 2015). The selected MNI coordinates for the seed regions were slightly different from the peak voxel coordinates to keep the MIN coordinates consistent across conditions and hemisphere. Detailed statistical values for selected ROIs and regional peak coordinates are displayed in Supplementary Table S1.

For the PPI analyses, the first eigenvariate of the time course within a 3-mm radius sphere in each seed region was extracted, adjusted for effects of interest (i.e., effects of conditions) as the physiological factor. Variance in the eigenvarite attributable to head motion was removed. The psychological factors were defined as the contrast between conditions (i.e., reward anticipation: large reward cue minus no reward cue; reward receipt: large reward hit minus no reward; infrequent reward omission: large reward miss minus large reward hit). The psychophysiological interaction factors were calculated as an interaction term of the physiological factors and psychological factors using the PPI toolbox in SPM 12. Finally, a GLM model with the PPI regressors (physiological, psychological, and interaction factors) of the seed region together with estimated movement parameters was generated. The effects of

psychophysiological interaction for each subject were estimated in the individual level GLM model and then specified in a group level GLM model together with other nuisance covariates (i.e., gender, pubertal stage, handedness and 7 dummy-coded acquisition sites).

Computational modeling of reward PE. To further examine brain activations associated with reward prediction error, a Rescorla-Wagner algorithm based Reinforcement Learning model was trained using reward cues and outcomes (Glascher and O'Doherty, 2010; Rescorla and Wagner, 1972). The model contained two internal variables: *Expected Value* (EV) representing the current estimation of the future expected rewards and *Prediction Error* (PE) representing the difference between the current reward and the expected value.

$$\mathbf{EV}_t = \mathbf{pGain}_t \times C_t$$

$$\mathbf{PE}_t = \mathbf{R}_t - \mathbf{EV}_t$$

$$\mathbf{pGain}_{t+1} = \mathbf{pGain}_t + \eta \times \frac{\mathbf{PE}_t}{\mathbf{C}_t}$$

Where C is the possible reward (0, 2 or 10 points), EV is expected value (EV), R is the actual reward, PE is prediction error, pGain is participant's subjective probability of obtaining the reward, η is learning rate and t corresponds to trial t. For a certain trial (t), each participant's subjective expected value (EV_t) is determined by the cue presented (C_t) and the participant's subjective possibility of obtaining it ($pGain_t$). The prediction error (PE_t) is defined as the difference between the actual received reward (R_t) and EV_t. Following reward receipt, the subjective probability of obtaining reward for next trial ($pGain_{t+1}$) is a sum of $pGain_t$ and PE_t divided by C_t, with the latter multiplied by the learning rate (η). The initial probability (pGain) was set to 0.5 and the learning rate was assumed to be same for all subjects and set to 0.7 (Glascher and O'Doherty, 2010; O'Doherty, et al., 2003). The EV and PE at each

trial for each subject were obtained from the record of rewards delivered during the task. In the individual GLM model, cue and outcome onsets were specified and parametrically modulated with trial-wise EV and PE respectively. The estimated head motion parameters were included as covariates. All regressors were convolved with the standard HRF in SPM12. Brain activations associated with reward PE were obtained by estimation of the parametric modulation effects of reward PE.

Gender and puberty analyses. Gender correlates (male vs. female) of adolescent brain response to reward processing were examined via two sample t-tests with pubertal stage, handedness and 7 dummy-coded acquisition sites included as nuisance covariates. For analyses of puberty, we focused on differences between early and late puberty stages (Menzies, et al., 2015). Given that males and females reach puberty at different ages, we compared male early puberty (PDS Stage 2, n = 91) vs. male late puberty (PDS Stage 4, n = 237) and female early puberty (PDS Stage 3 n = 80) vs. female late puberty (PDS Stage 5, n = 84).

Sensation Seeking. Sensation seeking scores were measured using a subscale of the SURPS (20 participants did not complete this measure and were not included in the sensation seeking analyses). Brain activation and functional connectivity during reward processing were correlated sensation seeking scores in a group level GLM model together with other nuisance covariates (i.e., gender, pubertal stage, handedness and 7 dummy-coded acquisition sites). For comparison with Cservenka et al. (2013), adolescents were further stratified into high sensation seekers and low sensation seekers (bottom 33% vs. top 33%; scores below 14 and above 16, respectively). Brain activation and functional connectivity during reward processing was compared between two groups using two sample t-test with other nuisance covariates regressed out.

RESULTS AND DISCUSSION

Table 1 displays sample characteristics. For the large reward condition, participants completed an average of 14.82 (SD = 2.47) reward hit trials and 7.17 (SD = 2.45) reward miss trials. For the small reward condition, participants completed an average of 14.85 (SD = 2.33) reward hit trials and 7.14 (SD = 2.33) reward miss trials. The different counts between hit and miss trials were due to an adaptive response interval designed to provide a successful outcome on 66% of trials. For the no reward condition participants completed an average of 22.01 (SD = 0.16) trials (including both hit and miss). The mean sensation seeking score was 13.95 (SD = 2.69; n = 1490) and the distribution of the sensation seeking scores is displayed in Supplementary Figure S1. The mean sensation seeking score for high sensation seeking group was 17.19 (SD = 1.25; n = 416), low sensation seeking group was 10.73 (SD = 1.38; n = 434).

[Insert Table 1 about here]

Reward Anticipation

Several regions had greater than 0.8 probability of positive activation during reward anticipation (see Figure 2A and Table 2A). Specifically, the activation of the midbrain included ventral tegmental area (VTA)/substantia nigra (SN) activation (left: peak probability: 1, MNI: -9, -16, -11; right: peak probability: 1, MNI: 9, -16, -11). No region had greater than 0.8 probability of negative activation. Figure 3A and Table 2B depict regions that showed significant changes in functional connectivity with thalamus during the anticipation of large reward versus no reward. Figure 3B and Table 2B depict regions that showed significant changes in functional connectivity with VS. Male adolescents had greater brain activity in bilateral putamen (left: t = 5.81, cluster size: 13, MNI: -30, -13, 4; right: t =

5.53, cluster size: 28, MNI: 30, -7, 1), right middle temporal gyrus (t = 6.13, cluster size: 22, MNI: 63, -16, -14) and right precuneus (t = 5.81, cluster size: 17, MNI: 9, -70, 40) than females in the reward anticipation (See Figure 2B). The sensation seeking analyses as well as other comparisons for gender and puberty, for either activation or connectivity, were non-significant.

[Insert Table 2 about here]

[Insert Figure 2 about here]

[Insert Figure 3 about here]

A previous study (Silverman, et al., 2015) examined activation likelihood estimation (ALE) for brain regions across 26 studies of adolescent reward processing and reported that the anticipation of positive rewards activated ventral striatum, OFC, insula, paracingulate gyrus, posterior cingulate gyrus and lateral occipital cortex, all of which were also activated in our study. In addition to the regions described by Silverman and colleagues, we also observed reliable activation in bilateral middle frontal gyrus, medial occipital cortex and parietal lobe. These additional observed regions are likely due to the use of a single standardized task across all participants. Silverman et al.'s (2015) findings were derived from a meta-analysis of different studies with an array of reward-processing tasks, whereas the activation patterns reported here are derived from the MID task alone using probability mapping on samples of 100 participants. Brain areas identified in our study, with 14-year-old adolescents, were previously reported in a meta-analysis of reward-related activation in healthy adults (Liu, et al., 2011).

With respect to the PPI analysis of reward anticipation, both thalamus and VS showed similar positive connections to anterior supplementary motor area (pre-SMA), dorsal anterior cingulate cortex (dACC), left anterior insula, and medial occipital lobe. The pre-SMA and dACC are related to the control of movement and action initiation (Asemi, et al., 2015; Srinivasan, et al., 2013), with evidence from a primate study showing that SMA and pre-SMA are targets of basal ganglia circuit (Akkal, et al., 2007). Therefore, the positive connectivity with pre-SMA and dACC likely reflects the increased motor preparation following the presentation of relatively large monetary cues. The anterior insula can relate to the interpretation of reward salience; that is, the insula is associated with the bottom-up processing of events such as the differential value of reward cues (Menon and Uddin, 2010). A previous meta-analysis showed that insula activity, particularly in left insula, relates to the motivational or affective salience of environmental events (Craig and Craig, 2009; Duerden, et al., 2013). Therefore, positive connectivity between VS/thalamus and left insula could indicate the integration of information about the motivational significance of cue. Thalamus and VS were both positively connected with medial occipital regions such as lingual gyrus, calcarine sulcus, cuneus, but negatively with inferior occipital lobe. This connectivity might represent value-driven attention capture whereby the evaluative strength of an event influences visual information processing (Anderson, 2016; Anderson, 2017). Specifically, the positive connections between seed and occipital regions could be attributed to differences in saliency between large reward and no reward stimulus.

Reward receipt: Positive activation

Bilateral vmPFC were the only regions to have greater than 0.8 probability of activation for reward receipt; see Figure 4A and Table 3A. Figure 4B and Table 3B report regions that showed significant changes in functional connectivity with vmPFC during the reward receipt. None of the comparisons for gender and puberty or with sensation seeking, with either activation or connectivity, were significant.

[Insert Table 3 about here]

[Insert Figure 4 about here]

In the present study, only vmPFC was positively reliably activated during reward receipt. This finding strongly supports the notion that activity in vmPFC represent outcome value (Peters and Büchel, 2010; Smith, et al., 2010), in both general and specific reward valuation (Levy and Glimcher, 2011), and especially, the magnitude during reward receipt (Diekhof, et al., 2012). For instance, the majority of previous studies using MID task reported the increased activation of vmPFC area in response to reward receipt (Bjork, et al., 2004; Bjork, et al., 2010; Knutson, et al., 2003); and the activity showed a positive correlation with the subjective pleasantness of different type of rewards: taste in the mouth and warmth on the hand (Grabenhorst, et al., 2010). Therefore, the activation of vmPFC would reflect the selectively active for reward magnitude. It is worth noting that the observed positive activation in vmPFC during reward receipt appears inconsistent with previous adolescent studies showing reliable VS activation during reward receipt (Shulman, et al., 2016), or absence of higher cortical activation related to reward (Silverman, et al., 2015). However, these differences may be explained by differences in the nature of the rewarding outcome. For example, Silverman et al.'s analysis focused on situations in which the reward outcome stage provided feedback about gains or

losses. In our study, the contrast for reward receipt involved a condition in which participants knew that the outcome would likely be a reward versus a condition in which it was known for certain that no reward would be provided. The observation of activity in vmPFC, but not VS, during reward receipt is consistent with previous adult findings (Knutson, et al., 2003; Rohe, et al., 2012) in this respect. Regarding the PPI results of reward receipt, bilateral vmPFC was negatively connected with bilateral insula and dorsal striatum. The anterior insula relates to the interpretation of reward salience (Menon and Uddin, 2010). Therefore, one possible explanation for vmPFC and insula connections would be that the connections may reflect the bottom-up processing of the differential value of reward outcome. Previous studies have dissociated roles of ventral and dorsal striatum and demonstrated that dorsal striatum is involved in maintaining information about the rewarding outcomes (Balleine, et al., 2007; O'Doherty, et al., 2004). The vmPFC and dorsal striatum connectivity may indicate learning of the reward results. Interestingly, left vmPFC was positively connected to right dlPFC. Rudorf and Hare (2014) showed that dlPFC encoded deviations from the default valuation context, and functional connectivity between vmPFC and dlPFC increased when choice context changes require a reweighting of the stimulus (Rudorf and Hare, 2014). Thus, functional coupling between right dlPFC and left vmPFC could indicate context-dependent valuation during reward receipt.

Reward receipt: Negative activation

As shown in Figure 5A and Table 4A, bilateral thalamus had greater than 0.8 probability of negative activation following reward receipt. Figure 5B and Table 4B depict regions that showed significant changes in functional connectivity with thalamus during reward receipt. None of the

comparisons for gender and puberty, or with sensation seeking, with either activation or connectivity, were significant.

[Insert Table 4 about here]

[Insert Figure 5 about here]

The negative activity following reward receipt is likely because the no reward condition could be regarded as a negative outcome when compared with large reward outcome. This could therefore contribute to increased activation of brain networks associated with negative emotion when compared with a large reward. For example, Santesso, et al., 2012 reported that negative feedback on MID task was associated with greater self-reported negative emotionality. Therefore, it is plausible that a no-reward outcome would be associated with increased thalamic activity given that thalamus serves as an information hub that conveys information between subcortical and cortical regions (Haber and Calzavara, 2009; Haber and Knutson, 2010). For instance, the negative connectivity between thalamus and prefrontal cortex when no reward is anticipated could reflect the regulation of the negative arousal associated given prefrontal cortex's role in regulation of emotional, motivational and cognitive arousal (Diamond, 2013; Hampshire, et al., 2010).

Infrequent reward omission

As shown in Figure 6A and Table 5A, bilateral VS showed greater than 0.8 probability of negative activation when a signaled reward was not delivered. No region had greater than 0.8 probability of positive activation. Figure 6B and Table 5B depict regions that showed significant changes in

functional connectivity with VS when a signaled reward was not delivered. None of comparisons for gender and puberty, or with sensation seeking, with either activation or connectivity, were significant.

[Insert Table 5 about here]

[Insert Figure 6 about here]

Bilateral VS showed negative activation when a signaled reward was not delivered, commensurate with previous studies (McClure, et al., 2003; O'Doherty, et al., 2003). These findings are concordant with previous evidence suggesting the fundamental role of VS lies in tracking the delivery of anticipated rewards and generation of PE signals: a process that is crucial to reinforcement learning (den Ouden, et al., 2012; Schultz, 2016). When comparing infrequent reward omission to frequent reward delivery, the PPI revealed bilateral VS positive connections with medial frontal gyrus, dACC, pre-SMA, precentral gyrus, putamen, insula, thalamus, precuneus, cuneus, lingual gyrus and calcarine sulcus. A previous review suggested that the processing of discrepancy between expected and unexpected rewards are widely associated with perception, attention, motivation and control network of the brain (den Ouden, et al., 2012), and the observed connections with VS are evidence for the involvement of this broader brain network. For example, the heightened connectivity between VS and prefrontal cortex during infrequent reward omission could reflect the adjustment of outcome expectancies during the process of reinforcement learning (van den Bos, et al., 2012). The more connection between VS and motor areas would reflect the inhibition of actions. The VS connections with lingual gyrus, calcarine sulcus, cuneus implies the involvement of the attention network in the processing of infrequent reward omission.

Computational modeling of reward PE

Table 5B and Figure 7A depict regions with greater than 0.8 probability of positive-activation associated parametric modulation of reward PE. Sensation Seeking scores were negatively correlated with parametric modulation of the reward PE in right inferior frontal gyrus (right IFG) (t = 4.88, MNI: 36, 38, 10). A comparison between high and low sensation seeking groups showed that adolescents with low sensation seeking scores had stronger right IFG activation associated with reward PE compared with adolescents with higher sensation seeking scores (t = 5.13, MNI: 36, 38, 10) (see Figure 7B). Comparisons for gender and puberty as well as other sensation seeking analyses, for either activation or connectivity, were non-significant.

[Insert Figure 7 about here]

The bilateral VS activation was correlated with parametric modulation of reward PE, consistent with a wealth of previous findings suggested that reward PE is primarily encoded in VS (Chase, et al., 2015; Garrison, et al., 2013). Sensation seeking was negatively correlated with right IFG activity following a reward PE (i.e., high sensation seeking adolescents had less right IFG activity for reward PE). Previous studies have reported right IFG involvement in processing of negative PE (Cservenka, et al., 2013; Meder, et al., 2016). For instance, participants with higher right IFG responses to negative PE were less likely to switch options in a probabilistic learning task (Meder, et al., 2016). As Cservenka and colleagues (2013) reported previously, high sensation seeking adolescents had greater deactivation following a no-win outcome (i.e., a larger negative PE). Here, we extend this finding by showing a correlation in the right IFG to both positive and negative PE effects, which we estimated using a

Rescrola-Wagner model. Interestingly, the correlation with sensation seeking was only observed with the computational model rather than the reward omission contrast. The lower right IFG activity observed in high sensation seeking adolescents may indicate that they allocate fewer attentional resources to the discrepancy between anticipated and actual outcome. We did not observe insula activity, unlike Cservenka et al. (2013); however, the cluster in the right IFG extended into anterior insula, albeit below the threshold for multiple comparison correction.

GENERAL DISCUSSION

In the present study, we examined neural activity associated with different stages of reward processing. We derived a map depicting the probability of a voxel being significant at a family-wise error rate corrected p-value under .05 for an aggregation of subsamples of 100 subjects, and we subsequently conducted PPI analyses. Our results showed that regions within the limbic system, salience network, attention network and motor areas showed activation and/or connections with seed regions in reward anticipation, reward receipt and infrequent reward omission. Within the different reward processing stages, we observed distinct patterns of activity. For example, thalamic connectivity differed by reward processing stage, with positive connectivity to motor-related areas only observed during reward anticipation. This work therefore refines our knowledge of thalamic activity during adolescent reward processing (Haber and Calzavara, 2009; Haber and Knutson, 2010). During the reward receipt stage, our probability analysis revealed markedly specific functional neuroanatomy: vmPFC was reliably activated during reward receipt but VS was reliably activated following a reward PE. These findings are consistent with results from statistical comparison showing a dissociation between reward receipt and PE (Rohe, et al., 2012). Studies have suggested that predicted amount of

reward associated with outcome of actions (goal values) is specifically encoded in vmPFC (Hare, et al., 2009; Hare, et al., 2008), whereas reward PE is coded in VS (Hare, et al., 2008; Peters and Buchel, 2010), findings that are strongly supported by our adolescent data.

Due to the large sample size, we could conduct gender-specific analyses. During reward anticipation, males had more activation in bilateral putamen, right middle temporal gyrus and precuneus compared with females. The comparisons for brain activation during reward processing between males and females suggest the basic reward system is broadly similar for both genders, with relatively minor differences for specific structures. A previous adult study suggested that men have stronger activation in left putamen in response to anticipated monetary reward (Spreckelmeyer, et al., 2009). Our results may provide evidence that the gender differences in left putamen activity associated with reward anticipation already exist in adolescence. Previous studies have shown that putamen, middle temporal gyrus and precuneus were associated with risk-taking behaviors (Goh, et al., 2016; Mitchell, et al., 2015). For instance, right putamen activity to a novel stimulus was positively correlated with following risk-taking choices (Mitchell, et al., 2015). Higher-risk sexual behaviors in adolescents are correlated with increased activation in right precuneus and temporal gyrus during receipt of social reward and increased precuneus functional connectivity with other regions (Eckstrand, et al., 2017). Therefore, a more nuanced understanding of the gender differences in brain regions associated with reward processing can contribute to our understanding of gender-specific vulnerabilities to problem behaviors during adolescence, such as adolescent males' tendency to engage in more risk-taking behaviors than females (Morrongiello and Rennie, 1998; Steinberg, 2004).

A growing literature has revealed the important role of pubertal development in adolescent reward processing (Blakemore, et al., 2010; Forbes, et al., 2011; Forbes, et al., 2010; Goddings, et al., 2014; Klapwijk, et al., 2013; Moore, et al., 2012; Urosevic, et al., 2014). Previous studies have revealed the positive correlation between sex hormone level and pubertal stage (Shirtcliff, et al., 2009), and sex hormone-levels, such as testosterone, was positively correlated with the striatum activation to a monetary reward for both boys and girls (Op de Macks, et al., 2011). Moreover, Forbes et al. (2010), in adolescents aged 11-13 years-old (pre-puberty vs mid-/late-puberty) found that male adolescents with higher testosterone level exhibited more striatal responses during reward anticipation and both adolescent males and females with higher testosterone level showed less striatal activity during reward outcome (Forbes, et al., 2010). In contrast with these studies, however, we did not observe any significant difference with voxel-wise FWE corrected threshold in separate comparisons of early vs. late pubertal development for males and females. The lack of puberty effects observed in the study was surprising especially when significant gender effects were observed from the same dataset. The Tanner stage is commonly used for measuring puberty in previous studies (Blakemore, et al., 2010; Goddings, et al., 2014), while other supplemental measurements such as hormone assays are recommended (Blakemore, et al., 2010). The lack of other measurement of pubertal stage, and variability in puberty stage which constrained our analysis in comparing males (Pubertal Stages 2 vs. 4) and females (Pubertal Stages 3 vs. 5) should be borne in mind when interpreting our results. Future studies with a wider age range and other measurements of pubertal stage may help to better understand puberty effects on the reward system. Pubertal effects on reward processing that survived cluster-wise FWE corrected threshold $p < 0.05$ are reported as supplementary results.

There are limitations to this study. First, our claims are limited to functional connectivity between brain regions, without any inference of directionality. Second, shape of the hemodynamic response function was assumed to be the same across brain regions and participants (O'Reilly, et al., 2012). Third, we assumed a fixed learning rate in the RW model. Future studies with individualized parameters may better capture the brain activation during reward processing.

CONCLUSION

Here, we investigated adolescent reward processing by examining brain activation and connectivity during reward anticipation and receipt on the MID task. For reward anticipation, activity was reliable across a wide range of regions, including bilateral ventral striatum, pallidum, insula, thalamus, hippocampus, cingulate cortex, midbrain, motor area and occipital gyrus. For reward receipt, only bilateral vmPFC and thalamus were reliably significant, with VS was reliably significant for infrequent reward omission and reward PE. The PPI results reflected the interaction between cortical and subcortical structures supporting different aspects of reward processing. Gender differences were consistently observed in left putamen, right precuneus and middle temporal gyrus during reward anticipation, while there were few effects of pubertal status on adolescent reward processing. Self-reported sensation seeking scores were negatively correlated with right IFG activity associated with parametric modulation of reward PE.

ACKNOWLEDGMENTS

This work received support from the following sources: Science Foundation Ireland (16/ERCD/3797), the European Union-funded FP6 Integrated Project IMAGEN (Reinforcement-related behaviour in normal brain function and psychopathology) (LSHM-CT- 2007-037286), the Horizon 2020 funded ERC Advanced Grant 'STRATIFY' (Brain network based stratification of reinforcement-related disorders) (695313), ERANID (Understanding the Interplay between Cultural, Biological and Subjective Factors in Drug Use Pathways) (PR-ST-0416-10004), BRIDGET (JPND: BRain Imaging, cognition Dementia and next generation GEnomics) (MR/N027558/1), the FP7 projects IMAGEMEND(602450; IMAging GEnetics for MENtal Disorders) and MATRICS (603016), the Innovative Medicine Initiative Project EU-AIMS (115300-2), the Medical Research Council Grant 'c-VEDA' (Consortium on Vulnerability to Externalizing Disorders and Addictions) (MR/N000390/1), the Swedish Research Council FORMAS, the Medical Research Council, the National Institute for Health Research (NIHR) Biomedical Research Centre at South London and Maudsley NHS Foundation Trust and King's College London, the Bundesministeriumfür Bildung und Forschung (BMBF grants 01GS08152; 01EV0711; eMED SysAlc01ZX1311A; Forschungsnetz AERIAL), the Deutsche Forschungsgemeinschaft (DFG grants SM 80/7-1, SM 80/7-2, SFB 940/1). Further support was provided by grants from: ANR (project AF12-NEUR0008-01 - WM2NA, and ANR-12-SAMA-0004), the Fondation de France, the Fondation pour la Recherche Médicale, the Mission Interministérielle de Lutte-contre-les-Drogues-et-les-Conduites-Addictives (MILDECA), the Assistance-Publique-Hôpitaux-de-Paris and INSERM (interface grant), Paris Sud University IDEX 2012, the National Institutes of Health, Science Foundation Ireland (16/ERCD/3797), U.S.A. (Axon, Testosterone and Mental Health during Adolescence, RO1 MH085772-01A1), and by NIH Consortium grant U54 EB020403, supported by a cross-NIH alliance that funds Big Data to Knowledge Centres of Excellence, Irish Research Council Postdoctoral Fellowship grant (GOIPD/2016/617), ZC is supported by China Scholarship Council.

CONFLICT OF INTEREST

Dr. Banaschewski served in an advisory or consultancy role for Actelion, Hexal Pharma, Lilly,Lundbeck, Medice, Novartis, Shire. He received conference support or speaker's fee by Lilly, Medice Novartis and Shire. He has been involved in clinical trials conducted by Shire & Viforpharma. He received royalities from Hogrefe, Kohlhammer, CIP Medien, Oxford University Press. The present work is unrelated to the above grants and relationships. Dr Barker has received funding for a PhD student and honoraria for teaching on scanner programming courses from General Electric Healthcare; he acts as a consultant for IXICO. Dr Walter received a speaker honorarium from Servier (2014).The other authors report no biomedical financial interests or potential conflicts of interest.

REFERENCES

Akkal, D., Dum, R.P., Strick, P.L. (2007) Supplementary motor area and presupplementary motor area: targets of basal ganglia and cerebellar output. J Neurosci, 27:10659-73.

Anderson, B.A. (2016) The attention habit: how reward learning shapes attentional selection. Ann N Y Acad Sci, 1369:24-39.

Anderson, B.A. (2017) Reward processing in the value-driven attention network: Reward signals tracking cue identity and location. Soc Cogn Affect Neurosci, 12:461-467.

Asemi, A., Ramaseshan, K., Burgess, A., Diwadkar, V.A., Bressler, S.L. (2015) Dorsal anterior cingulate cortex modulates supplementary motor area in coordinated unimanual motor behavior. Front Hum Neurosci, 9:309.

Azim, E., Mobbs, D., Jo, B., Menon, V., Reiss, A.L. (2005) Sex differences in brain activation elicited by humor. Proc Natl Acad Sci U S A, 102:16496-501.

Balleine, B.W., Delgado, M.R., Hikosaka, O. (2007) The role of the dorsal striatum in reward and decision-making. J Neurosci, 27:8161-5.

Bjork, J.M., Knutson, B., Fong, G.W., Caggiano, D.M., Bennett, S.M., Hommer, D.W. (2004) Incentive-elicited brain activation in adolescents: similarities and differences from young adults. J Neurosci, 24:1793-802.

Bjork, J.M., Smith, A.R., Chen, G., Hommer, D.W. (2010) Adolescents, adults and rewards: Comparing motivational neurocircuitry recruitment using fMRI. PLoS One, 5:e11440.

Blakemore, S.J., Burnett, S., Dahl, R.E. (2010) The role of puberty in the developing adolescent brain. Hum Brain Mapp, 31:926-33.

Button, K.S., Ioannidis, J.P., Mokrysz, C., Nosek, B.A., Flint, J., Robinson, E.S., Munafo, M.R. (2013) Power failure: why small sample size undermines the reliability of neuroscience. Nat Rev Neurosci, 14:365-76.

Casey, B. (2015) Beyond simple models of self-control to circuit-based accounts of adolescent behavior. Annu Rev Psychol, 66:295-319.

Casey, B., Cannonier, T., Conley, M. I., Cohen, A. O., Barch, D. M., Heitzeg, M. M., . . . Workgroup, A. I. A. (2018). The Adolescent Brain Cognitive Development (ABCD) study: Imaging acquisition across 21 sites. Dev Cogn Neurosci, 32, 43-54.

Chase, H.W., Kumar, P., Eickhoff, S.B., Dombrovski, A.Y. (2015) Reinforcement learning models and their neural correlates: An activation likelihood estimation meta-analysis. Cogn Affect Behav Neurosci, 15:435-59.

Craig, A.D., Craig, A. (2009) How do you feel--now? The anterior insula and human awareness. Nat Rev Neurosci, 10.

Cservenka, A., Herting, M.M., Seghete, K.L.M., Hudson, K.A., Nagel, B.J. (2013) High and low sensation seeking adolescents show distinct patterns of brain activity during reward processing. Neuroimage, 66:184-193.

den Ouden, H.E., Kok, P., de Lange, F.P. (2012) How prediction errors shape perception, attention, and motivation. Front Psychol, 3:548.

Diamond, A. (2013) Executive functions. Annu Rev Psychol, 64:135-68.

Diekhof, E.K., Kaps, L., Falkai, P., Gruber, O. (2012) The role of the human ventral striatum and the medial orbitofrontal cortex in the representation of reward magnitude - an activation likelihood estimation meta-analysis of neuroimaging studies of passive reward expectancy and outcome processing. Neuropsychologia, 50:1252-66.

Duerden, E.G., Arsalidou, M., Lee, M., Taylor, M.J. (2013) Lateralization of affective processing in the insula. Neuroimage, 78:159-75.

Eckstrand, K.L., Choukas-Bradley, S., Mohanty, A., Cross, M., Allen, N.B., Silk, J.S., Jones, N.P., Forbes, E.E. (2017) Heightened activity in social reward networks is associated with adolescents' risky sexual behaviors. Dev Cogn Neurosci, 27:1-9.

Ernst, M., Torrisi, S., Balderston, N., Grillon, C., Hale, E.A. (2015) fMRI functional connectivity applied to adolescent neurodevelopment. Annu Rev Clin Psychol, 11:361-77.

Forbes, E.E., Phillips, M.L., Silk, J.S., Ryan, N.D., Dahl, R.E. (2011) Neural systems of threat processing in adolescents: Role of pubertal maturation and relation to measures of negative affect. Dev Neuropsychol, 36:429-52.

Forbes, E.E., Ryan, N.D., Phillips, M.L., Manuck, S.B., Worthman, C.M., Moyles, D.L., Tarr, J.A., Sciarrillo, S.R., Dahl, R.E. (2010) Healthy adolescents' neural response to reward: associations with puberty, positive affect, and depressive symptoms. J Am Acad Child Adolesc Psychiatry, 49:162-72 e1-5.

Friston, K., Buechel, C., Fink, G., Morris, J., Rolls, E., Dolan, R. (1997) Psychophysiological and modulatory interactions in neuroimaging. Neuroimage, 6:218-229.

Garrison, J., Erdeniz, B., Done, J. (2013) Prediction error in reinforcement learning: a meta-analysis of neuroimaging studies. Neurosci Biobehav Rev, 37:1297-310.

Glascher, J.P., O'Doherty, J.P. (2010) Model-based approaches to neuroimaging: combining reinforcement learning theory with fMRI data. Wiley Interdiscip Rev Cogn Sci, 1:501-510.

Goddings, A.L., Mills, K.L., Clasen, L.S., Giedd, J.N., Viner, R.M., Blakemore, S.J. (2014) The influence of puberty on subcortical brain development. Neuroimage, 88:242-51.

Goh, J.O., Su, Y.S., Tang, Y.J., McCarrey, A.C., Tereshchenko, A., Elkins, W., Resnick, S.M. (2016) Frontal, striatal, and medial temporal sensitivity to value distinguishes risk-taking from risk-aversive older adults during decision making. J Neurosci, 36:12498-12509.

Grabenhorst, F., D'Souza, A.A., Parris, B.A., Rolls, E.T., Passingham, R.E. (2010) A common neural scale for the subjective pleasantness of different primary rewards. Neuroimage, 51:1265-74.

Haase, L., Green, E., Murphy, C. (2011) Males and females show differential brain activation to taste when hungry and sated in gustatory and reward areas. Appetite, 57:421-34.

Haber, S.N., Calzavara, R. (2009) The cortico-basal ganglia integrative network: the role of the thalamus. Brain Res Bull, 78:69-74.

Haber, S.N., Knutson, B. (2010) The reward circuit: Linking primate anatomy and human imaging. Neuropsychopharmacology, 35:4-26.

Hampshire, A., Chamberlain, S.R., Monti, M.M., Duncan, J., Owen, A.M. (2010) The role of the right inferior frontal gyrus: inhibition and attentional control. Neuroimage, 50:1313-9.

Hare, T.A., Camerer, C.F., Rangel, A. (2009) Self-control in decision-making involves modulation of the vmPFC valuation system. Science, 324:646-8.

Hare, T.A., O'Doherty, J., Camerer, C.F., Schultz, W., Rangel, A. (2008) Dissociating the role of the orbitofrontal cortex and the striatum in the computation of goal values and prediction errors. J Neurosci, 28:5623-30.

Hawes, S.W., Chahal, R., Hallquist, M.N., Paulsen, D.J., Geier, C.F., Luna, B. (2017) Modulation of reward-related neural activation on sensation seeking across development. Neuroimage, 147:763-771.

Jia, T., Macare, C., Desrivieres, S., Gonzalez, D.A., Tao, C., Ji, X., Ruggeri, B., Nees, F., Banaschewski, T., Barker, G.J., Bokde, A.L., Bromberg, U., Buchel, C., Conrod, P.J., Dove, R., Frouin, V., Gallinat, J., Garavan, H., Gowland, P.A., Heinz, A., Ittermann, B., Lathrop, M., Lemaitre, H., Martinot, J.L., Paus, T., Pausova, Z., Poline, J.B., Rietschel, M., Robbins, T., Smolka, M.N., Muller, C.P., Feng, J., Rothenfluh, A., Flor, H., Schumann, G., Consortium, I. (2016) Neural basis of reward anticipation and its genetic determinants. Proc Natl Acad Sci U S A, 113:3879-84.

Jollans, L., Zhipeng, C., Icke, I., Greene, C., Kelly, C., Banaschewski, T., Bokde, A.L., Bromberg, U., Buchel, C., Cattrell, A., Conrod, P.J., Desrivieres, S., Flor, H., Frouin, V., Gallinat, J., Garavan, H., Gowland, P., Heinz, A., Ittermann, B., Martinot, J.L., Artiges, E., Nees, F., Papadopoulos Orfanos, D., Paus, T., Smolka, M.N., Walter, H., Schumann, G., Whelan, R. (2016) Ventral Striatum Connectivity During Reward Anticipation in Adolescent Smokers. Dev Neuropsychol, 41:6-21.

Jurk, S., Kuitunen-Paul, S., Kroemer, N.B., Artiges, E., Banaschewski, T., Bokde, A.L., Büchel, C., Conrod, P., Fauth-Bühler, M., Flor, H. (2015) Personality and substance Use: psychometric evaluation and validation of the Substance Use Risk Profile Scale (SURPS) in English, Irish, French, and German adolescents. Alcohol Clin Exp Res, 39:2234-2248.

Karoly, H.C., Bryan, A.D., Weiland, B.J., Mayer, A., Dodd, A., Feldstein Ewing, S.W. (2015) Does incentive-elicited nucleus accumbens activation differ by substance of abuse? An examination with adolescents. Dev Cogn Neurosci, 16:5-15.

Klapwijk, E.T., Goddings, A.L., Burnett Heyes, S., Bird, G., Viner, R.M., Blakemore, S.J. (2013) Increased functional connectivity with puberty in the mentalising network involved in social emotion processing. Horm Behav, 64:314-22.

Knutson, B., Fong, G.W., Bennett, S.M., Adams, C.M., Hommer, D. (2003) A region of mesial prefrontal cortex tracks monetarily rewarding outcomes: characterization with rapid event-related fMRI. Neuroimage, 18:263-72.

Knutson, B., Westdorp, A., Kaiser, E., Hommer, D. (2000) FMRI visualization of brain activity during a monetary incentive delay task. Neuroimage, 12:20-7.

Levy, D.J., Glimcher, P.W. (2011) Comparing apples and oranges: using reward-specific and reward-general subjective value representation in the brain. J Neurosci, 31:14693-707.

Liu, X., Hairston, J., Schrier, M., Fan, J. (2011) Common and distinct networks underlying reward valence and processing stages: A meta-analysis of functional neuroimaging studies. Neurosci Biobehav Rev, 35:1219-36.

Lorenz, R.C., Gleich, T., Beck, A., Pohland, L., Raufelder, D., Sommer, W., Rapp, M.A., Kuhn, S., Gallinat, J. (2014) Reward anticipation in the adolescent and aging brain. Hum Brain Mapp, 35:5153-65.

Ma, I., van Holstein, M., Mies, G.W., Mennes, M., Buitelaar, J., Cools, R., Cillessen, A.H.N., Krebs, R.M., Scheres, A. (2016) Ventral striatal hyperconnectivity during rewarded interference control in adolescents with ADHD. Cortex, 82:225-236.

McClure, S.M., Berns, G.S., Montague, P.R. (2003) Temporal prediction errors in a passive learning task activate human striatum. Neuron, 38:339-46.

Meder, D., Madsen, K.H., Hulme, O., Siebner, H.R. (2016) Chasing probabilities—Signaling negative and positive prediction errors across domains. NeuroImage, 134:180-191.

Memetovic, J., Ratner, P.A., Gotay, C., Richardson, C.G. (2016) Examining the relationship between personality and affect-related attributes and adolescents' intentions to try smoking using the Substance Use Risk Profile Scale. Addict Behav, 56:36-40.

Menon, V., Uddin, L.Q. (2010) Saliency, switching, attention and control: A network model of insula function. Brain Struct Funct, 214:655-67.

Menzies, L., Goddings, A.L., Whitaker, K.J., Blakemore, S.J., Viner, R.M. (2015) The effects of puberty on white matter development in boys. Dev Cogn Neurosci, 11:116-28.

Mitchell, S., Gao, J., Hallett, M., Voon, V. (2015) The role of novelty in risk seeking behaviour. J Neurol Neurosurg Psychiatry, 86:e3.

Moore, W.E., 3rd, Pfeifer, J.H., Masten, C.L., Mazziotta, J.C., Iacoboni, M., Dapretto, M. (2012) Facing puberty: Associations between pubertal development and neural responses to affective facial displays. Soc Cogn Affect Neurosci, 7:35-43.

Morrongiello, B.A., Rennie, H. (1998) Why do boys engage in more risk taking than girls? The role of attributions, beliefs, and risk appraisals. J Pediatr Psychol, 23:33-43.

Munro, C.A., McCaul, M.E., Wong, D.F., Oswald, L.M., Zhou, Y., Brasic, J., Kuwabara, H., Kumar, A., Alexander, M., Ye, W., Wand, G.S. (2006) Sex differences in striatal dopamine release in healthy adults. Biol Psychiatry, 59:966-74.

O'Doherty, J., Dayan, P., Schultz, J., Deichmann, R., Friston, K., Dolan, R.J. (2004) Dissociable roles of ventral and dorsal striatum in instrumental conditioning. Science, 304:452-4.

O'Doherty, J.P., Dayan, P., Friston, K., Critchley, H., Dolan, R.J. (2003) Temporal difference models and reward-related learning in the human brain. Neuron, 38:329-37.

O'Reilly, J.X., Woolrich, M.W., Behrens, T.E., Smith, S.M., Johansen-Berg, H. (2012) Tools of the trade: psychophysiological interactions and functional connectivity. Soc Cogn Affect Neurosci, 7:604-9.

Op de Macks, Z.A., Gunther Moor, B., Overgaauw, S., Guroglu, B., Dahl, R.E., Crone, E.A. (2011) Testosterone levels correspond with increased ventral striatum activation in response to monetary rewards in adolescents. Dev Cogn Neurosci, 1:506-16.

Peters, J., Büchel, C. (2010) Neural representations of subjective reward value. Behav Brain Res, 213:135-141.

Peters, J., Bromberg, U., Schneider, S., Brassen, S., Menz, M., Banaschewski, T., Conrod, P.J., Flor, H., Gallinat, J., Garavan, H., Heinz, A., Itterman, B., Lathrop, M., Martinot, J.L., Paus, T., Poline, J.B., Robbins, T.W., Rietschel, M., Smolka, M., Strohle, A., Struve, M., Loth, E., Schumann, G., Buchel, C., Consortium, I. (2011) Lower ventral striatal activation during reward anticipation in adolescent smokers. Am J Psychiatry, 168:540-9.

Peters, J., Buchel, C. (2010) Neural representations of subjective reward value. Behav Brain Res, 213:135-41.

Petersen, A. C., Crockett, L., Richards, M., & Boxer, A. (1988). A self-report measure of pubertal status: Reliability, validity, and initial norms. Journal of youth and adolescence, 17(2), 117-133.

Rescorla, R.A., Wagner, A.R. (1972) A theory of Pavlovian conditioning: Variations in the effectiveness of reinforcement and nonreinforcement. Classical conditioning II: Current research and theory, 2:64-99.

Rohe, T., Weber, B., Fliessbach, K. (2012) Dissociation of BOLD responses to reward prediction errors and reward receipt by a model comparison. Eur J Neurosci, 36:2376-82.

Rudorf, S., Hare, T.A. (2014) Interactions between dorsolateral and ventromedial prefrontal cortex underlie context-dependent stimulus valuation in goal-directed choice. J Neurosci, 34:15988-96.

Santesso, D.L., Bogdan, R., Birk, J.L., Goetz, E.L., Holmes, A.J., Pizzagalli, D.A. (2012) Neural responses to

negative feedback are related to negative emotionality in healthy adults. Soc Cogn Affect Neurosci, 7:794-803.

Scheres, A., Milham, M.P., Knutson, B., Castellanos, F.X. (2007) Ventral striatal hyporesponsiveness during reward anticipation in attention-deficit/hyperactivity disorder. Biol Psychiatry, 61:720-4.

Schlauch, R.C., Crane, C.A., Houston, R.J., Molnar, D.S., Schlienz, N.J., Lang, A.R. (2015) Psychometric evaluation of the Substance Use Risk Profile Scale (SURPS) in an inpatient sample of substance users using cue-reactivity methodology. J Psychopathol Behav Assess, 37:231-246.

Schneider, S., Brassen, S., Bromberg, U., Banaschewski, T., Conrod, P., Flor, H., Gallinat, J., Garavan, H., Heinz, A., Martinot, J.L., Nees, F., Rietschel, M., Smolka, M.N., Strohle, A., Struve, M., Schumann, G., Buchel, C., Consortium, I. (2012a) Maternal interpersonal affiliation is associated with adolescents' brain structure and reward processing. Transl Psychiatry, 2:e182.

Schneider, S., Peters, J., Bromberg, U., Brassen, S., Miedl, S.F., Banaschewski, T., Barker, G.J., Conrod, P., Flor, H., Garavan, H., Heinz, A., Ittermann, B., Lathrop, M., Loth, E., Mann, K., Martinot, J.L., Nees, F., Paus, T., Rietschel, M., Robbins, T.W., Smolka, M.N., Spanagel, R., Strohle, A., Struve, M., Schumann, G., Buchel, C., Consortium, I. (2012b) Risk taking and the adolescent reward system: a potential common link to substance abuse. Am J Psychiatry, 169:39-46.

Schultz, W. (2016) Dopamine reward prediction error coding. Dialogues Clin Neurosci, 18:23-32.

Schumann, G., Loth, E., Banaschewski, T., Barbot, A., Barker, G., Buchel, C., Conrod, P.J., Dalley, J.W., Flor, H., Gallinat, J., Garavan, H., Heinz, A., Itterman, B., Lathrop, M., Mallik, C., Mann, K., Martinot, J.L., Paus, T., Poline, J.B., Robbins, T.W., Rietschel, M., Reed, L., Smolka, M., Spanagel, R., Speiser, C., Stephens, D.N., Strohle, A., Struve, M., consortium, I. (2010) The IMAGEN study: Reinforcement-related behaviour in normal brain function and psychopathology. Mol Psychiatry, 15:1128-39.

Shirtcliff, E.A., Dahl, R.E., Pollak, S.D. (2009) Pubertal development: correspondence between hormonal and physical development. Child Dev, 80:327-37.

Shulman, E.P., Smith, A.R., Silva, K., Icenogle, G., Duell, N., Chein, J., Steinberg, L. (2016) The dual systems model: Review, reappraisal, and reaffirmation. Dev Cogn Neurosci, 17:103-17.

Silverman, M.H., Jedd, K., Luciana, M. (2015) Neural networks involved in adolescent reward processing: An activation likelihood estimation meta-analysis of functional neuroimaging studies. Neuroimage, 122:427-39.

Smith, D.V., Hayden, B.Y., Truong, T.K., Song, A.W., Platt, M.L., Huettel, S.A. (2010) Distinct value signals in anterior and posterior ventromedial prefrontal cortex. J Neurosci, 30:2490-5.

Spreckelmeyer, K.N., Krach, S., Kohls, G., Rademacher, L., Irmak, A., Konrad, K., Kircher, T., Grunder, G. (2009) Anticipation of monetary and social reward differently activates mesolimbic brain structures in men and women. Soc Cogn Affect Neurosci, 4:158-65.

Srinivasan, L., Asaad, W.F., Ginat, D.T., Gale, J.T., Dougherty, D.D., Williams, Z.M., Sejnowski, T.J., Eskandar, E.N. (2013) Action initiation in the human dorsal anterior cingulate cortex. PLoS One, 8:e55247.

Steinberg, L. (2004) Risk taking in adolescence: what changes, and why? Ann N Y Acad Sci, 1021:51-58.

Stringaris, A., Vidal-Ribas Belil, P., Artiges, E., Lemaitre, H., Gollier-Briant, F., Wolke, S., Vulser, H., Miranda, R., Penttila, J., Struve, M., Fadai, T., Kappel, V., Grimmer, Y., Goodman, R., Poustka, L., Conrod, P., Cattrell, A., Banaschewski, T., Bokde, A.L., Bromberg, U., Buchel, C., Flor, H., Frouin, V., Gallinat, J., Garavan, H., Gowland, P., Heinz, A., Ittermann, B., Nees, F., Papadopoulos, D., Paus, T., Smolka, M.N.,

Walter, H., Whelan, R., Martinot, J.L., Schumann, G., Paillere-Martinot, M.L., Consortium, I. (2015) The Brain's Response to Reward Anticipation and Depression in Adolescence: Dimensionality, Specificity, and Longitudinal Predictions in a Community-Based Sample. Am J Psychiatry, 172:1215-23.

Tahmasebi, A.M., Artiges, E., Banaschewski, T., Barker, G.J., Bruehl, R., Buchel, C., Conrod, P.J., Flor, H., Garavan, H., Gallinat, J., Heinz, A., Ittermann, B., Loth, E., Mareckova, K., Martinot, J.L., Poline, J.B., Rietschel, M., Smolka, M.N., Strohle, A., Schumann, G., Paus, T., Consortium, I. (2012) Creating probabilistic maps of the face network in the adolescent brain: A multicentre functional MRI study. Hum Brain Mapp, 33:938-57.

Urosevic, S., Collins, P., Muetzel, R., Lim, K.O., Luciana, M. (2014) Pubertal status associations with reward and threat sensitivities and subcortical brain volumes during adolescence. Brain Cogn, 89:15-26.

van den Bos, W., Cohen, M.X., Kahnt, T., Crone, E.A. (2012) Striatum-medial prefrontal cortex connectivity predicts developmental changes in reinforcement learning. Cereb Cortex, 22:1247-55.

van den Bos, W., Rodriguez, C.A., Schweitzer, J.B., McClure, S.M. (2015) Adolescent impatience decreases with increased frontostriatal connectivity. Proc Natl Acad Sci U S A, 112:E3765-74.

Weiland, B.J., Welsh, R.C., Yau, W.Y., Zucker, R.A., Zubieta, J.K., Heitzeg, M.M. (2013) Accumbens functional connectivity during reward mediates sensation-seeking and alcohol use in high-risk youth. Drug Alcohol Depend, 128:130-9.

Woicik, P.A., Stewart, S.H., Pihl, R.O., Conrod, P.J. (2009) The substance use risk profile scale: A scale measuring traits linked to reinforcement-specific substance use profiles. Addict Behav, 34:1042-1055.

Xia, M., Wang, J., He, Y. (2013) BrainNet Viewer: A network visualization tool for human brain connectomics. PLoS One, 8:e68910.

Yacubian, J., Glascher, J., Schroeder, K., Sommer, T., Braus, D.F., Buchel, C. (2006) Dissociable systems for gain- and loss-related value predictions and errors of prediction in the human brain. J Neurosci, 26:9530-7.

Yang, Y., Narr, K.L., Baker, L.A., Joshi, S.H., Jahanshad, N., Raine, A., Thompson, P.M. (2015) Frontal and striatal alterations associated with psychopathic traits in adolescents. Psychiatry Res, 231:333-40.

Zuckerman, M. (2014) Sensation seeking (psychology revivals): beyond the optimal level of arousal. London: Psychology Press.

Figure 1. Stimuli in the Monetary Incentive Delay (MID) task. Cues signaling the task condition (no reward, small reward, large reward) were displayed for 4000 to 4500 ms. The response and feedback phase lasted a total of 2 s, during which target was displayed for 250-400 ms and feedback was displayed for 1450 ms. Trials were separated by 3500-4150 ms intertrial interval.

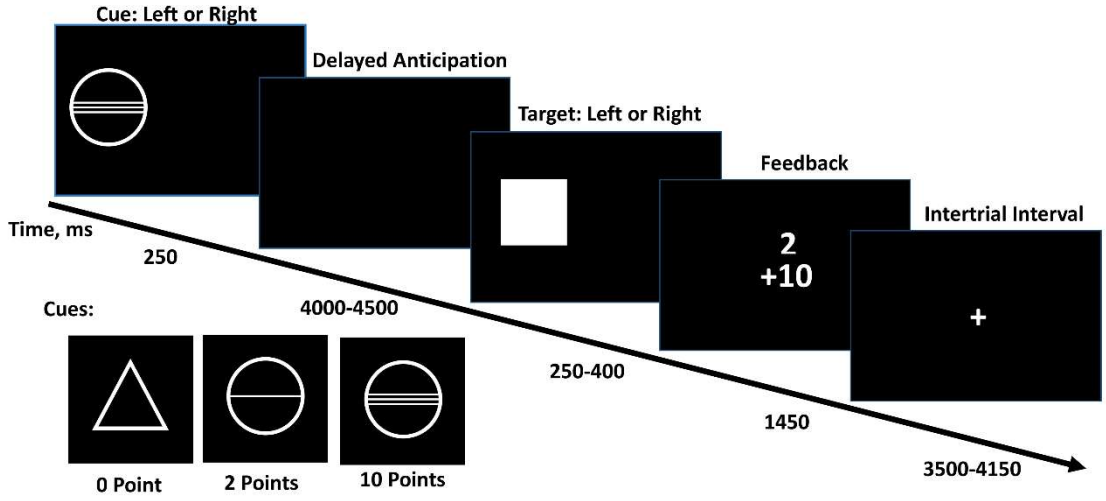

Figure 2. A: Probabilistic map of positive activation during reward anticipation. The color bar denotes the probability of activation. B: Regions that showed more activity for male compared with female adolescents during reward anticipation. The color bar denotes *t* values.

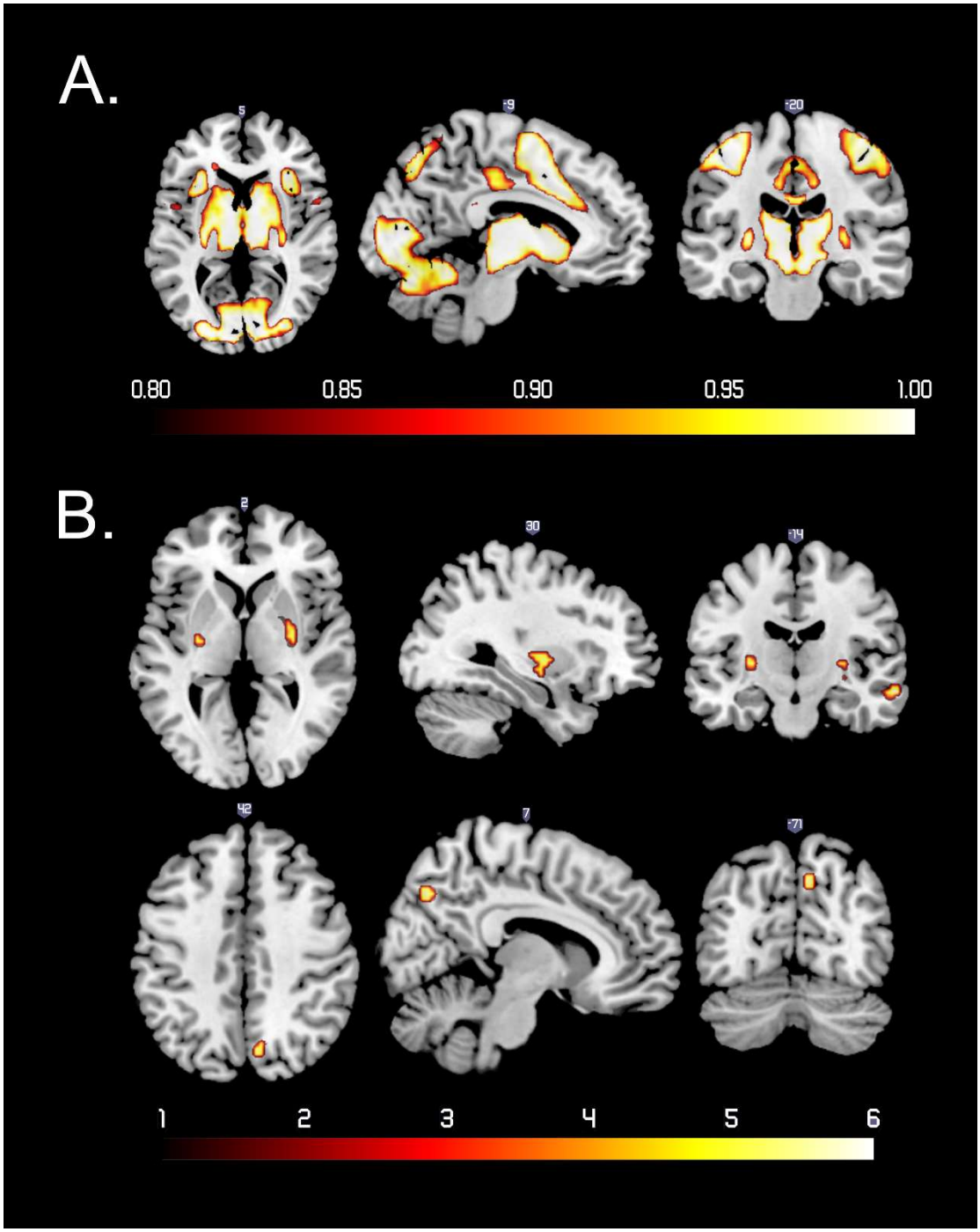

Figure 3. A: Regions that showed significant changes in functional connectivity with left and right thalamus during reward anticipation. B: Regions that showed significant changes in functional connectivity with left and right VS during reward anticipation. The connectivity maps were generated using BrainNet Viewer (Xia, et al., 2013). Nodes drawn in red indicates regions showed positive connectivity with the seed region. Blue indicates negative connectivity. Unified MNI coordinates are used for the display purpose. The MNI coordinates used for plots are shown in the Supplementary Materials. ANG = Angular Gyrus, ACG = Anterior Cingulate Gyri, CAL = Calcarine, CAU = Caudate, CUN = Cuneus, IFGoperc = Inferior Frontal Gyrus, Opercular Part, IFGtriang = Inferior Frontal Gyrus, Triangular Part, IOG = Inferior Occipital Gyrus, IPL = Inferior Parietal Gyrus, INS = Insula, LING = Lingual Gyrus, DCG = Median Cingulate Gyri, MFG = Middle Frontal Gyrus, PoCG = Postcentral Gyrus, PreCG = Precentral Gyrus, PUT = Putamen, SFGdor = Superior Frontal Gyrus, ORBsupmed = Superior Frontal Gyrus, Medial Orbital, STG = Superior Temporal Gyrus, SMA = Supplementary Motor Area, THA = Thalamus; L = Left, R = Right.

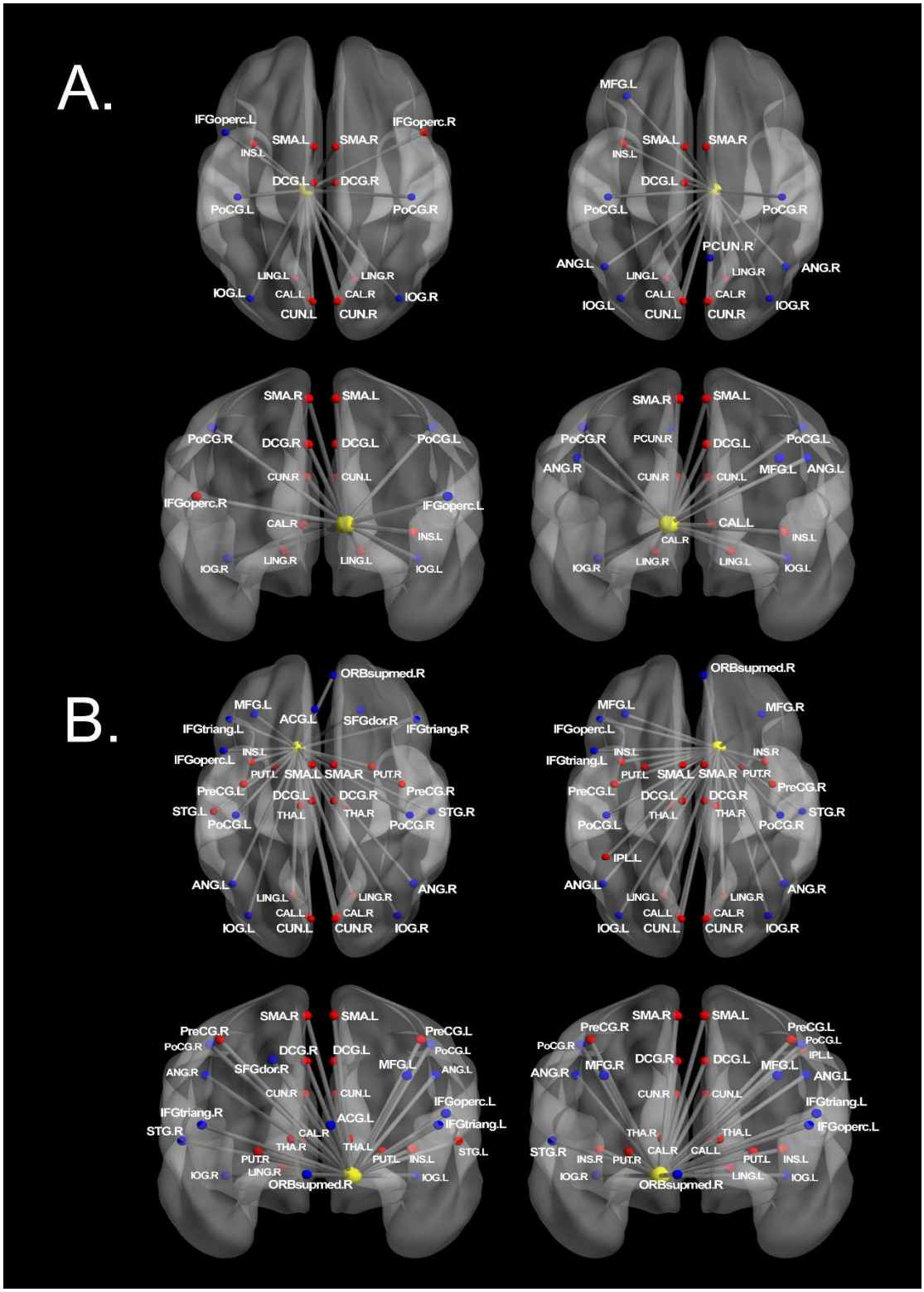
A.
IFGoperc.L
IFGoperc.R
SMA.L
SMA.R
INS.L
DCG.L
DCG.R
PoCG.L
PoCG.R
LING.L
LING.R
IOG.L
CAL.L
CAL.R
IOG.R
CUN.L
CUN.R
MFG.L
PCUN.R
ANG.L
ANG.R
PCUN.L
MFG.R
ANG.L
B.
ORBsupmed.R
ACG.L
SFGdor.R
IFGtriang.L
IFGtriang.R
INS.R
PUT.L
PUT.R
PreCG.L
PreCG.R
STG.L
STG.R
THA.L
THA.R
IPL.L
ORBsupmed.R

Figure 4. A. Probabilistic map for positive activation during reward receipt. The color bar denotes the probability of activation. B. Regions that showed significant changes in functional connectivity with vmPFC during reward receipt. Nodes drawn in red indicates regions showed positive connectivity with the seed region. Blue indicates negative connectivity. Unified MNI coordinates are used for the display purpose. The MNI coordinates used for plots are shown in the Supplementary Materials. ACG = Anterior Cingulate Gyri, CAL = Calcarine, CAU = Caudate, CUN = Cuneus, DS = Dorsal Striatum, HIP = Hippocampus, IFGoperc = Inferior Frontal Gyrus, Opercular Part, IFGtriang = Inferior Frontal Gyrus, Triangular Part, IOG = Inferior Occipital Gyrus, INS = Insula, LING = Lingual Gyrus, DCG = Median Cingulate Gyri, MFG = Middle Frontal Gyrus, MOG = Middle Occipital Gyrus, PreCG = Precentral Gyrus, PCUN = Precuneus, PUT = Putamen, SMA = Supplementary Motor Area, THA = Thalamus; L = Left, R = Right.

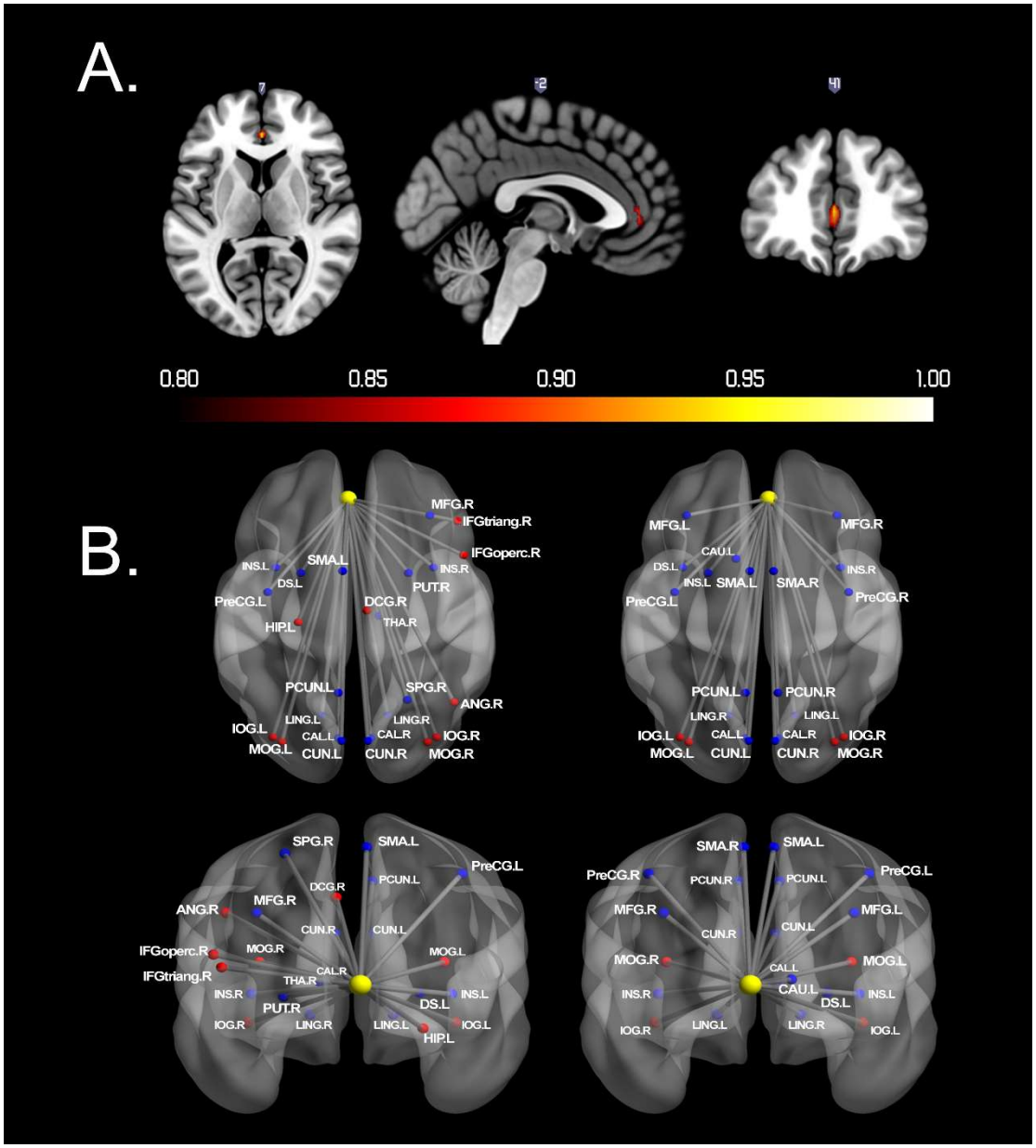
A.
0.80
0.85
0.90
0.95
1.00
B.
MFG.R
IFGtriang.R
IFGoperc.R
SMA.L
INS.L
INS.R
DS.L
PUT.R
PreCG.L
DCG.R
THA.R
HIP.L
PCUN.L
SPG.R
ANG.R
LING.L
LING.R
IOG.L
CAL.L
CAL.R
IOG.R
MOG.L
CUN.L
CUN.R
MOG.R
MFG.L
CAU.L
SMA.R
PreCG.R
PCUN.R
SPG.L
SMA.L
PreCG.L
DCG.L
PCUN.L
MFG.L
ANG.L
CUN.L
MOG.L
IFGoperc.L
IFGtriang.L
THA.L
INS.L
PUT.L
DS.L
IOG.L
LING.L
HIP.L
SMA.R
PreCG.R
PCUN.R
MFG.R
CUN.R
MOG.R
CAL.L
CAU.L
INS.R
DS.L
IOG.R
LING.R

Figure 5. A: Probabilistic map for negative activation during reward receipt. The color bar denotes the probability of activation. B: Regions that showed significant changes in functional connectivity with thalamus during reward receipt. Nodes drawn in red indicates regions showed positive connectivity with the seed region. Blue indicates negative connectivity. Unified MNI coordinates are used for the display purpose. The MNI coordinates used for plots are shown in the Supplementary Materials. ANG = Angular Gyrus, HIP = Hippocampus, IFGtriang = Inferior Frontal Gyrus, Triangular Part, IOG = Inferior Occipital Gyrus, IPL = Inferior Parietal Gyrus, INS = Insula, DCG = Median Cingulate Gyri, MFG = Middle Frontal Gyrus, PoCG = Postcentral Gyrus, PCUN = Precuneus, ROL = Rolandic Operculum, SFGdor = Superior Frontal Gyrus, SFGmed = Superior Frontal Gyrus, Medial, STG = Superior Temporal Gyrus, THA = Thalamus; L = Left, R = Right.

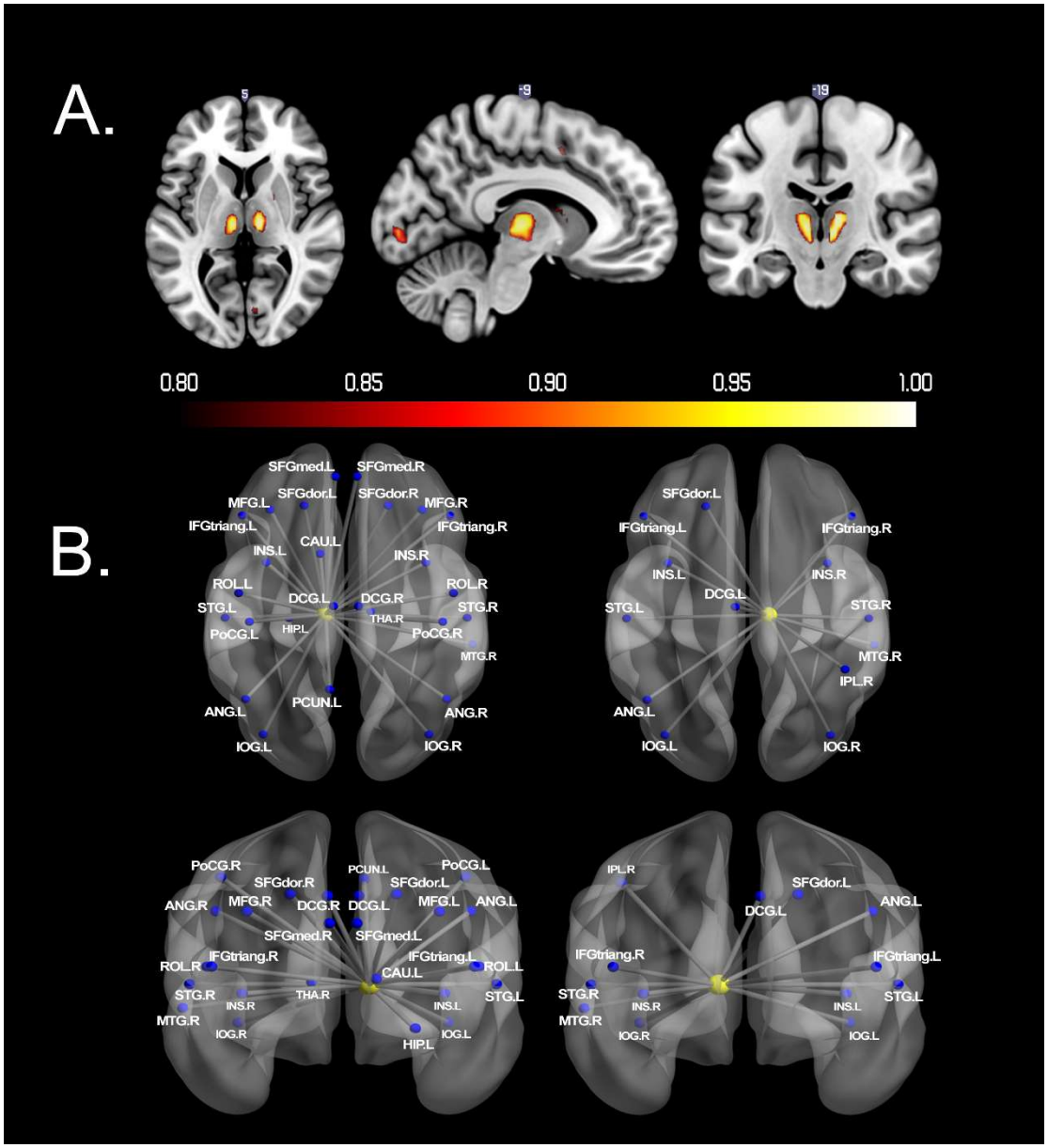
A.
5
-9
-19
0.80
0.85
0.90
0.95
1.00
B.
SFGmed.L
SFGmed.R
SFGdor.L
SFGdor.R
MFG.L
MFG.R
IFGtriang.L
IFGtriang.R
CAU.L
INS.L
INS.R
ROL.L
ROL.R
DCG.L
DCG.R
STG.L
STG.R
THA.R
HIP.L
PoCG.L
PoCG.R
MTG.R
ANG.L
PCUN.L
ANG.R
IOG.L
IOG.R
SFGdor.L
IFGtriang.L
IFGtriang.R
INS.L
INS.R
DCG.L
STG.L
STG.R
MTG.R
IPL.R
ANG.L
IOG.L
IOG.R
PoCG.R
PCUN.L
PoCG.L
SFGdor.R
SFGdor.L
ANG.R
MFG.R
DCG.R
DCG.L
MFG.L
ANG.L
SFGmed.R
SFGmed.L
IFGtriang.R
IFGtriang.L
ROL.R
CAU.L
ROL.L
STG.R
INS.R
THA.R
INS.L
STG.L
MTG.R
IOG.R
IOG.L
HIP.L
IPL.R
SFGdor.L
ANG.L
DCG.L
IFGtriang.R
IFGtriang.L
STG.R
INS.R
INS.L
STG.L
MTG.R
IOG.R
IOG.L

Figure 6. A: Probabilistic map for negative activation during infrequent reward omission. The color bar denotes the probability of activation. B: Regions that showed significant changes in functional connectivity with VS during infrequent reward omission. Nodes drawn in red indicates regions showed positive connectivity with the seed region. Blue indicates negative connectivity. Unified MNI coordinates are used for the display purpose. The MNI coordinates used for plots are shown in the Supplementary Materials. CAL = Calcarine, CAU = Caudate, CUN = Cuneus, IOG = Inferior Occipital Gyrus, INS = Insula, LING = Lingual Gyrus, DCG = Median Cingulate Gyri, MFG = Middle Frontal Gyrus, MTG = Middle Temporal Gyrus, PoCG = Postcentral Gyrus, PCG = Posterior Cingulate Gyrus, PreCG = Precentral Gyrus, PCUN = Precuneus, PUT = Putamen, SMA = Supplementary Motor Area, SMG = Supramarginal Gyrus; L = Left, R = Right.

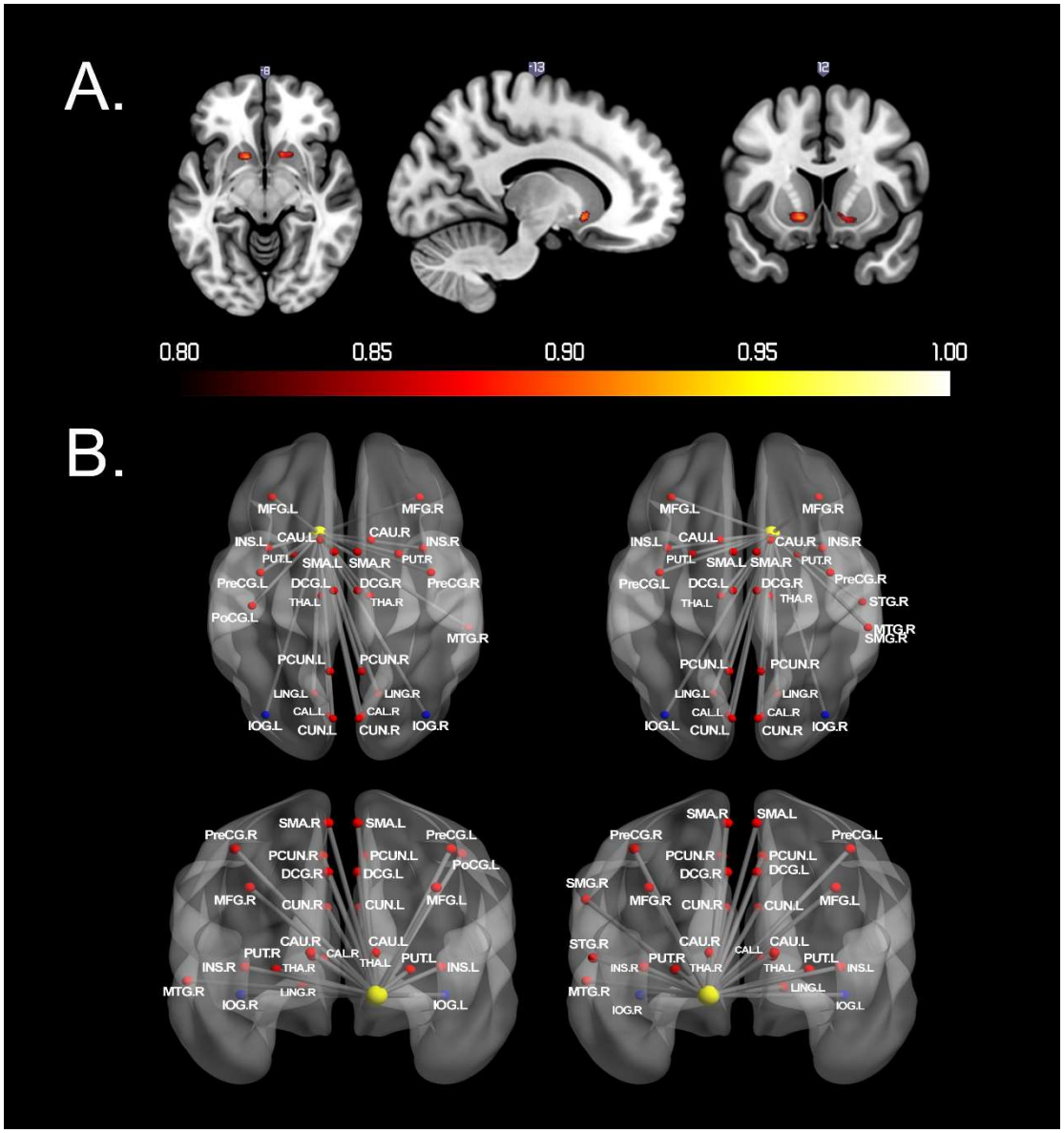
A.
-8
-13
12
0.80
0.85
0.90
0.95
1.00
B.
MFG.L
MFG.R
INS.L
CAU.L
CAU.R
INS.R
PUT.L
SMA.L
SMA.R
PUT.R
PreCG.L
DCG.L
DCG.R
PreCG.R
THA.L
THA.R
PoCG.L
MTG.R
PCUN.L
PCUN.R
LING.L
LING.R
CAL.L
CAL.R
IOG.L
CUN.L
CUN.R
IOG.R
STG.R
SMG.R
SMA.R
SMA.L
PreCG.R
PreCG.L
PCUN.R
PCUN.L
DCG.R
DCG.L
PoCG.L
MFG.R
CUN.R
CUN.L
MFG.L
CAU.R
CAU.L
PUT.R
CAL.R
THA.L
PUT.L
INS.R
THA.R
INS.L
MTG.R
LING.R
IOG.R
IOG.L
SMG.R
STG.R
CAL.L
LING.L

Figure 7. A: Probabilistic map of positive activation in response to reward prediction error (PE). The color bar denotes the probability of activation. B: Left: Regions that showed different activity associated with reward PE between low sensation seeking group vs. high sensation seeking group. The color bar denotes *t* values. Right: Mean and standard error of right IFG activity for high and low sensation seeking groups. Right IFG activity from the contrast image was extracted from a 3-mm spherical ROI at MNI coordinates: 36, 38, 10.

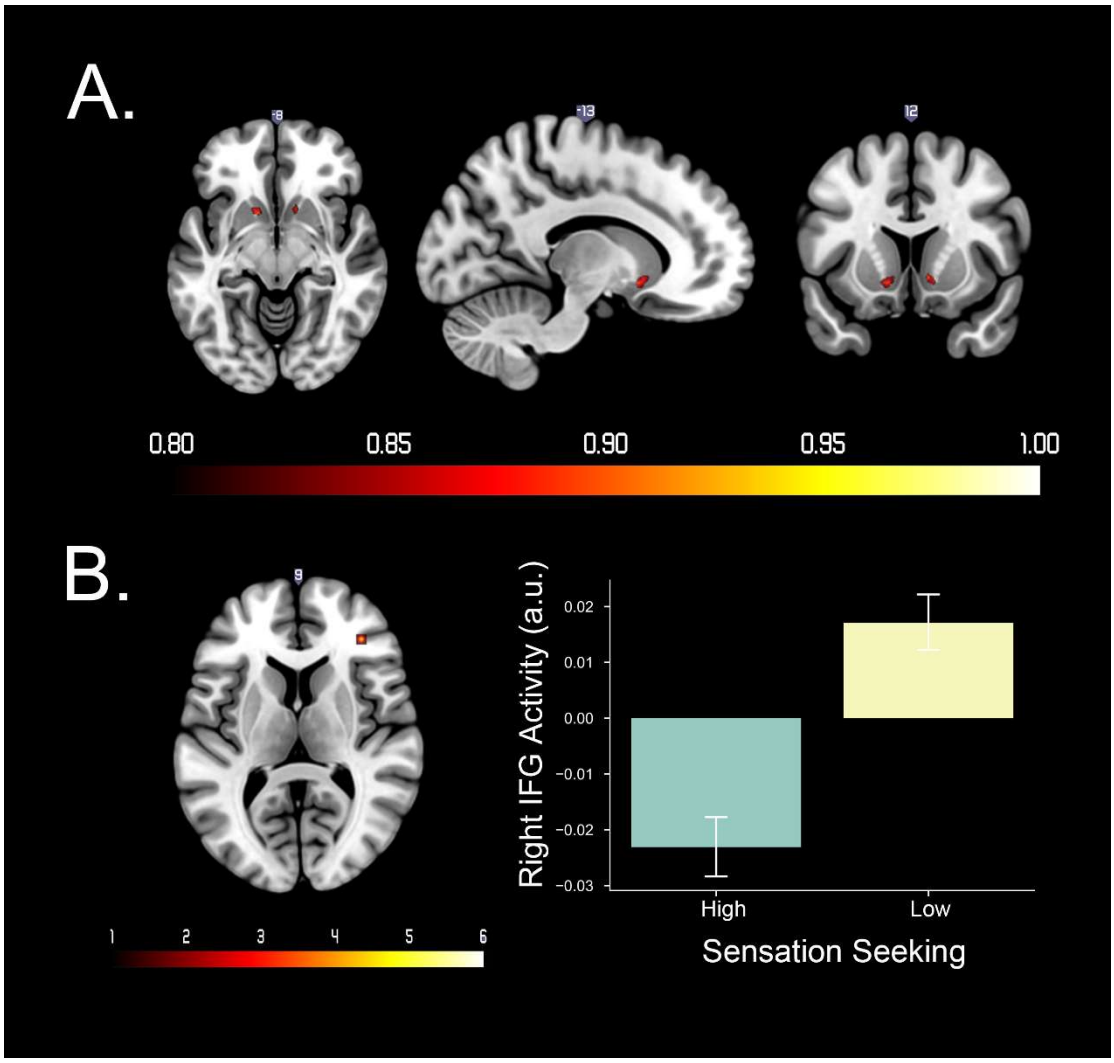

Table 1. Participant Characteristics.

	Whole sample	**Male**	**Female**
Sample size, n	1510	715	795
Handedness, Left/Right, n	166/1344	89/626	77/718
Age, years, mean(SD)	14.54(0.44)	14.53(0.43)	14.55(0.45)
Verbal Comprehension, mean(SD)	111.13(14.41)	112.61(14.20)	109.79(14.47)
Perceptual Reasoning, mean(SD)	108.48(14.23)	108.43(14.62)	108.52(13.87)
Pubertal Stage, n			
Pre-pubertal (1)	9	9	0
Beginning pubertal (2)	92	91	1
Mid-pubertal (3)	448	368	80
Advanced pubertal (4)	867	237	630
Post-pubertal (5)	94	10	84

Table 2. A. Regions that showed probability of positive activation above 0.8 during reward anticipation. The number of voxels exceeding the threshold for probabilities of .8, .9 and 1 from each cluster are presented, in addition to the maximum *t* value and corresponding MNI coordinates. B. Regions that showed significant changes in functional connectivity with thalamus and VS during reward anticipation. Main regions within the cluster, cluster size, peak *t*-value within the cluster as well as the corresponding MNI coordinates for the clusters with cluster size above 10 are shown in the table. (L = left; R = right; L/R=bilateral)

Region	**Cluster Size (voxels)**			**Peak**	**MNI (x,y,z)**		
A. Probabilistic map							
	1	**>0.9**	**>0.8**	**P (*t*)**			
Superior Frontal Gyrus (L)	5	31	49	1 (32.54)	-30	-7	67
Superior Frontal Gyrus (R)	7	61	88	1 (32.17)	36	-4	64
Middle Frontal Gyrus (L)	6	15	39	1 (33.01)	-30	-4	52
Middle Frontal Gyrus (R)	24	35	56	1 (32.82)	33	-4	55
Olfactory Cortex (L)	3	6	6	1 (34.37)	-15	8	-14
Olfactory Cortex (R)	3	4	6	1 (34.51)	18	8	-14
Thalamus (L)	132	168	183	1 (49.00)	-12	-19	10
Thalamus (R)	126	159	165	1 (49.37)	12	-13	7
VS(L)	5	6	8	1 (42.13)	-12	14	-8
VS (R)	4	5	6	1 (44.92)	12	14	-8
Insula (L)	15	71	97	1 (34.77)	-30	26	4
Insula (R)	21	74	87	1 (35.10)	33	29	4
Caudate (L)	39	62	83	1 (47.13)	-9	11	-2
Caudate (R)	57	94	112	1 (48.41)	9	11	1
Pallidum (L)	7	24	27	1 (40.07)	-12	8	-2
Pallidum (R)	6	20	23	1 (35.14)	12	5	-2
Putamen (L)	32	93	119	1 (42.49)	-15	11	-8
Putamen (R)	17	65	101	1 (42.29)	18	17	-8
Midbrain (L)	95	133	157	1 (44.04)	-6	-25	-5
Midbrain (R)	77	130	147	1 (47.04)	6	-25	-5
Anterior Cingulate Gyri (L)	6	28	42	1 (30.05)	-6	20	28
Anterior Cingulate Gyri (R)	4	28	53	1 (29.71)	6	23	28
Supplementary Motor Area (L)	129	180	199	1 (43.14)	-6	5	49
Supplementary Motor Area (R)	131	205	225	1 (42.71)	6	5	49
Precentral Gyrus (L)	132	245	303	1 (36.72)	-36	-25	61
Precentral Gyrus (R)	109	214	276	1 (34.88)	42	-16	52
Precuneus (L)	6	45	72	1 (30.62)	-12	-73	46
Precuneus (R)	8	40	69	1 (30.65)	15	-73	46
Median Cingulate Gyri (L)	58	119	144	1 (38.15)	-6	8	40
Median Cingulate Gyri (R)	73	155	213	1 (39.86)	6	11	43

Postcentral Gyrus (L)	142	219	258	1 (36.49)	-42	-19	52
Postcentral Gyrus (R)	22	131	202	1 (33.20)	42	-22	52
Inferior Parietal Gyrus (L)	14	149	200	1 (32.09)	-30	-49	49
Inferior Parietal Gyrus (R)	0	20	48	0.98 (25.85)	30	-49	49
Superior Parietal Gyrus (L)	35	139	181	1 (30.20)	-15	-70	52
Superior Parietal Gyrus (R)	5	53	101	1 (31.55)	12	-70	52
Cuneus (L)	2	11	27	1 (28.85)	0	-82	16
Cuneus (R)	2	17	37	1 (28.89)	18	-91	10
Lingual Gyrus (L)	58	110	133	1 (37.85)	-12	-88	-8
Lingual Gyrus (R)	49	99	137	1 (39.63)	15	-88	-5
Calcarine (L)	102	140	155	1 (40.21)	-12	-91	-5
Calcarine (R)	62	111	143	1 (40.99)	15	-91	-2
Fusiform Gyrus (L)	13	31	54	1 (35.59)	-18	-88	-8
Fusiform Gyrus (R)	6	24	38	1 (31.22)	24	-82	-14
Inferior Occipital Gyrus (L)	24	36	56	1 (36.92)	-30	-88	-8
Inferior Occipital Gyrus (R)	7	22	38	1 (32.66)	33	-85	-2
Middle Occipital Gyrus (L)	71	128	172	1 (38.17)	-27	-91	1
Middle Occipital Gyrus (R)	9	53	90	1 (32.60)	33	-85	1
Superior Occipital Gyrus (L)	17	50	68	1 (34.56)	-12	-94	4
Superior Occipital Gyrus (R)	2	45	69	1 (29.31)	24	-88	10
Cerebellum (L)	178	562	756	1 (35.83)	-33	-52	-32
Cerebellum (R)	222	537	698	1 (34.86)	18	-52	-23
B. Connectivity map							
Thalamus (L) Positive							
Lingual Gyrus (L/R)		1208		9.63	9	-88	16
Calcarine (L/R)							
Cuneus (L/R)							
Supplementary Motor Area (L/R)		174		7.16	3	2	64
Dorsal cingulate gyri (L/R)							
Insula (L)		25		5.76	-33	14	10
Inferior Frontal Gyrus, Opercular Part (R)		10		5.46	33	23	-8
Insula (L)		13		5.38	-45	2	4
Thalamus (L) Negative							
Inferior Occipital Gyrus (L)		137		15.66	-30	-88	-8
Inferior Occipital Gyrus (R)		165		15.04	21	-88	-11
Postcentral Gyrus (R)		83		6.93	57	-7	28
Postcentral Gyrus (L)		67		6.55	-51	-10	31
Inferior Frontal Gyrus, Opercular Part (L)		26		5.99	-48	17	34
Thalamus (R) Positive							
Lingual Gyrus (L/R)		708		9.02	9	-91	16
Calcarine (L/R)							
Cuneus (L/R)							
Supplementary Motor Area (L/R)		50		6.66	0	2	61
Insula (L)		33		6.23	-33	17	10
Dorsal cingulate gyri (L)		24		5.66	-6	14	37

Insula (R)	11	5.73	48	5	1
Putamen (R)	16	5.57	21	11	1
Calcarine (R)	10	5.07	24	-64	13
Thalamus (R) Negative					
Inferior Occipital Gyrus (L)	195	16.76	-27	-88	-8
Inferior Occipital Gyrus (R)	171	15.18	33	-85	-8
Postcentral Gyrus (L)	119	7.91	-57	-10	34
Postcentral Gyrus (R)	108	7.3	60	-7	28
Middle Frontal Gyrus (L)	73	6.25	-42	14	31
Angular Gyrus (R)	67	6.14	39	-70	40
Precuneus (R)	31	6.01	6	-61	49
Postcentral Gyrus (L)	23	5.99	-36	-31	67
Angular Gyrus (L)	68	5.72	-33	-67	37
Middle Frontal Gyrus (L)	15	5.36	-33	17	55
VS (L) Positive					
Lingual Gyrus (L/R)	1375	9.78	9	-88	22
Calcarine (L/R)					
Cuneus (L/R)					
Supplementary Motor Area (L/R)	612	9.77	3	5	61
Median Cingulate Gyri (L/R)					
Precentral Gyrus (R)	84	8.02	45	-7	52
Insula (L)	40	7.67	-30	20	10
Precentral Gyrus (L)	84	7.37	-42	-7	55
Putamen (R)	85	7.33	21	14	-2
Median Cingulate Gyri (L)	38	6.84	-12	-22	40
Insula (L)	48	6.55	-45	11	1
Thalamus (R)	43	6.16	6	-13	-2
Putamen (L)	26	5.44	-21	14	-2
Thalamus (L)	16	6.05	-6	-22	4
Superior Temporal Gyrus (L)	11	5.66	51	11	-2
VS (L) Negative					
Inferior Occipital Gyrus (L)	103	15.26	-21	-91	-5
Inferior Occipital Gyrus (R)	104	13.72	33	-85	-8
Angular Gyrus (L)	67	7.16	-42	-73	37
Postcentral Gyrus (L)	45	7.14	-54	-7	28
Postcentral Gyrus (R)	83	6.99	57	-7	28
Inferior Frontal Gyrus, Triangular Part (R)	54	6.56	48	38	16
Inferior Frontal Gyrus, Opercular Part (L)	51	6.52	-45	17	34
Middle Frontal Gyrus (L)	59	6.40	-30	23	55
Superior Frontal Gyrus, Medial Orbital (R)	41	5.99	6	47	-11
Superior Frontal Gyrus (R)	37	5.86	30	26	55
Inferior Frontal Gyrus, Triangular Part (L)	31	5.71	-45	35	10
Angular Gyrus (R)	19	6.02	45	-67	40
Superior Temporal Gyrus (R)	17	5.77	57	-10	4

Inferior Frontal Gyrus, Triangular Part (L)	12	5.36	-54	26	7
Anterior Cingulate Gyri (L)	11	4.98	-6	38	1
VS (R) Positive					
Supplementary Motor Area (L/R)	884	10.44	0	-1	61
Median Cingulate Gyri (L/R)					
Lingual Gyrus (L/R)	1595	10.41	9	-88	22
Calcarine (L/R)					
Cuneus (L/R)					
Precentral Gyrus (R)	122	8.16	42	-10	55
Insula (L)	119	7.85	-33	20	10
Thalamus (L)	58	7.36	-6	-22	7
Precentral Gyrus (L)	78	6.98	-36	-7	46
Thalamus (R)	89	6.66	6	-16	1
Insula (R)	61	6.42	33	26	7
Putamen (R)	73	6.30	21	11	-2
Putamen (L)	57	6.09	-12	8	-2
Precentral Gyrus (L)	13	6.45	-51	-1	43
Inferior Parietal Gyrus (L)	11	5.46	-24	-52	52
VS (R) Negative					
Inferior Occipital Gyrus (L)	107	14.61	-30	-88	-8
Inferior Occipital Gyrus (R)	98	14.51	33	-85	-8
Angular Gyrus (L)	38	7.33	-42	-73	34
Postcentral Gyrus (R)	45	6.54	57	-7	31
Angular Gyrus (R)	28	6.08	48	-67	37
Postcentral Gyrus (L)	21	5.66	-54	-10	31
Superior Temporal Gyrus (R)	18	5.96	60	-7	4
Superior Frontal Gyrus, Medial Orbital (R)	18	5.68	9	50	-11
Middle Frontal Gyrus (R)	11	5.68	30	20	58
Inferior Frontal Gyrus, Opercular Part (L)	13	5.61	-39	17	31
Middle Frontal Gyrus (L)	14	5.31	-30	23	55
Inferior Frontal Gyrus, Triangular Part (L)	15	5.30	-45	38	-2

Table 3. A. Regions that showed probability of positive activation above 0.8 during reward receipt. The number of voxels exceeding the threshold for probabilities of .8, .9 and 1 from each cluster are presented, in addition to the maximum *t* value and corresponding MNI coordinates. B. Regions that showed significant changes in functional connectivity with vmPFC during reward receipt. Main regions within the cluster, cluster size, peak *t*-value within the cluster as well as the corresponding MNI coordinates for the clusters with cluster size above 10 are shown in the table. (L = left; R = right; L/R=bilateral)

Region	Cluster Size (voxels)			Peak	MNI (x,y,z)		
A. Probabilistic map							
	1	**>0.9**	**>0.8**	**P (*t*)**			
vmPFC (L)	0	5	19	0.97 (25.83)	0	38	10
vmPFC (R)	0	0	5	0.88 (23.53)	3	41	7
B. Connectivity map							
vmPFC (L) Positive							
Middle Occipital Gyrus (L)		302		18.48	-27	-88	-11
Inferior Occipital Gyrus (L)							
Middle Occipital Gyrus (R)		302		18.44	21	-88	-11
Inferior Occipital Gyrus (R)							
Hippocampus (L)		12		7.15	24	-28	-2
Angular Gyrus (R)		94		6.86	30	-70	28
Inferior Frontal Gyrus, Triangular Part (R)		24		6.02	54	23	22
Median Cingulate Gyri (R)		19		5.58	3	-22	31
Inferior Frontal Gyrus, Opercular Part (R)		12		5.22	51	14	34
vmPFC (L) Negative							
Cuneus (L/R)		674		9.94	-9	-76	-5
Calcarine (L/R)							
Lingual Gyrus (L/R)							
Supplementary Motor Area (L)		299		8.91	-6	2	58
Insula (L)		153		6.83	-21	8	10
Dorsal striatum (L)							
Precentral Gyrus (L)		103		6.67	-42	-10	49
Insula (R)		19		6.83	36	14	7
Middle Frontal Gyrus (R)		20		6.26	39	-7	52
Precuneus (L)		23		5.98	-9	-58	61
Thalamus (R)		17		5.71	-15	-28	22
Calcarine (R)		27		5.62	33	-55	1
Lingual Gyrus (R)		11		5.54	18	-46	-8

Putamen (R)	12	5.33	24	8	7
Superior Parietal Gyrus (R)	10	5.19	18	-58	61
vmPFC (R) Positive					
Middle Occipital Gyrus (L)	265	18.3	-27	-88	-11
Inferior Occipital Gyrus (L)					
Middle Occipital Gyrus (R)	278	17.67	21	-88	-11
Inferior Occipital Gyrus (R)					
Middle Occipital Gyrus (R)	51	6.64	30	-70	28
vmPFC (R) Negative					
Cuneus (L/R)	852	10.04	-6	-79	-5
Calcarine (L/R)					
Lingual Gyrus (L/R)					
Supplementary Motor Area (L/R)	522	9.2	-6	5	55
Precentral Gyrus (L)					
Precuneus (L)	80	7.24	-9	-58	61
Precentral Gyrus (R)	61	7.12	42	-4	52
Insula (L)	54	6.38	-39	11	7
Middle Frontal Gyrus (L)	29	6.3	-33	38	31
Precuneus (R)	44	6.24	9	-52	58
Dorsal striatum (L)	29	6.13	-21	8	10
Caudate (L)	15	5.82	3	8	13
Insula (R)	10	5.78	36	14	7
Middle Frontal Gyrus (R)	22	5.64	30	35	31

Table 4. A. Regions that showed probability of negative activation above 0.8 during reward receipt. The number of voxels exceeding the threshold for probabilities of .8, .9 and 1 from each cluster are presented, in addition to the maximum *t* value and corresponding MNI coordinates. B. Regions that showed significant changes in functional connectivity with thalamus during reward receipt. Main regions within the cluster, cluster size, peak *t*-value within the cluster as well as the corresponding MNI coordinates for the clusters with cluster size above 10 are shown in the table. (L = left; R = right; L/R=bilateral)

Region	**Cluster Size (voxels)**			**Peak**	**MNI (x,y,z)**		
A. Probabilistic map							
	1	**>0.9**	**>0.8**	**P (*t*)**			
Thalamus (L)	2	47	67	1.00 (29.97)	-6	-22	-2
Thalamus (R)	3	41	57	1.00 (28.18)	9	-19	10
Supramarginal Gyrus (R)	5	27	44	1.00 (26.94)	60	-46	37
Supplementary Motor Area (L)	0	2	13	0.95 (25.90)	-6	2	52
Supplementary Motor Area (R)	2	19	31	1.00 (27.55)	6	5	55
Angular Gyrus (R)	0	4	10	0.95 (26.53)	60	-52	28
Middle Frontal Gyrus (L)	0	0	17	0.88 (23.98)	-36	41	31
Caudate (R)	0	1	9	0.91 (24.22)	12	2	16
Calcarine (L)	0	1	16	0.91 (23.86)	-9	-88	-5
Calcarine (R)	0	0	7	0.86 (23.79)	9	-82	1
Lingual Gyrus (R)	0	1	6	0.93 (24.73)	9	-79	-2
B. Connectivity map							
Thalamus (L) Negative							
Inferior Occipital Gyrus (L)		214		10.77	-30	-88	-8
Inferior Occipital Gyrus (R)		260		10.36	21	-88	-11

Superior Temporal Gyrus (R)	869	9.31	48	-13	16
Insula (R)					
Rolandic Operculum (R)					
Postcentral Gyrus (R)					
Superior Temporal Gyrus (L)	1619	9.09	0	-25	13
Rolandic Operculum (L)					
Inferior Frontal Gyrus, Triangular Part (L)					
Insula (L)					
Postcentral Gyrus (L)					
Angular Gyrus (L)	103	7.89	-48	-67	34
Superior Frontal Gyrus (L/R)	536	7.65	-18	35	46
Superior Frontal Gyrus, Medial (L/R)					
Middle Frontal Gyrus (L)					
Cerebellum (L)	30	6.86	-3	-43	-26
Cerebellum (R)	33	6.84	24	-34	-26
Postcentral Gyrus (L)	61	6.51	-30	-40	61
Precuneus (L)	70	6.42	-3	-55	7
Cerebellum (L)	15	6.39	-27	-37	-29
Middle Frontal Gyrus (R)	23	6.28	36	23	49
Postcentral Gyrus (R)	26	6.26	24	-40	67
Inferior Frontal Gyrus, Triangular Part (R)	83	6.26	48	41	19
Superior Frontal Gyrus (R)	43	6.05	12	41	52
Middle Temporal Gyrus (R)	16	5.98	60	-10	-14
Postcentral Gyrus (R)	65	5.94	42	-34	61
Angular Gyrus (R)	44	5.89	36	-73	37
Thalamus (R)	18	5.88	18	-31	-2
Insula (R)	22	5.88	21	29	13
Thalamus (R)	13	5.76	24	-28	16
Median Cingulate Gyri (L/R)	40	5.67	6	-4	37
Caudate (L)	13	5.47	18	11	22
Hippocampus (L)	13	5.45	-33	-37	-5
Thalamus (R) Negative					

Inferior Occipital Gyrus (L)	118	10.42	-30	-88	-8
Inferior Occipital Gyrus (R)	195	9.32	21	-88	-11
Superior Temporal Gyrus (R)	377	8.03	54	-28	16
Insula (R)					
Superior Temporal Gyrus (L)	519	6.84	-54	-7	4
Inferior Frontal Gyrus, Triangular Part (L)					
Insula (L)					
Cerebelum (R)	25	6.31	27	-34	-26
Inferior Frontal Gyrus, Triangular Part (R)	64	6.02	51	38	16
Angular Gyrus (L)	11	5.74	-48	-67	34
Median Cingulate Gyri (L)	19	5.66	0	-4	37
Inferior Parietal Gyrus (R)	10	5.47	54	-31	55
Middle Temporal Gyrus (R)	15	5.40	66	-37	1
Superior Frontal Gyrus (L)	23	5.31	-15	38	46

Table 5. A. Regions that showed probability of negative activation above 0.8 during infrequent reward omission. The number of voxels exceeding the threshold for probabilities of .8, .9 and 1 from each cluster are presented, in addition to the maximum *t* value and corresponding MNI coordinates. B. Regions that showed probability of positive activation above 0.8 in response to the parametric modulation of reward PE. C. Regions that showed significant changes in functional connectivity with VS during infrequent reward omission. Main regions within the cluster, cluster size, peak *t*-value within the cluster as well as the corresponding MNI coordinates for the clusters with cluster size above 10 are shown in the table. (L = left; R = right; L/R=bilateral)

Region	**Cluster Size (voxels)**			**Peak**	**MNI (x,y,z)**		
A. Probabilistic map							
	1	**>0.9**	**>0.8**	**P (*t*)**			
VS (L)	0	0	1	0.89 (24.11)	-12	14	-8
VS (R)	0	1	2	0.92 (25.13)	12	14	-8
Putamen (L)	0	3	7	0.91 (23.79)	-18	14	-5
Putamen (R)	0	1	4	0.92 (24.20)	18	14	-8
Inferior Parietal Gyrus (L)	0	0	7	0.88 (24.73)	-30	-70	43
B. Probabilistic map for reward PE							
VS (L)	0	0	2	0.87 (33.52)	-12	14	-8
VS (R)	0	0	2	0.90 (35.70)	12	14	-8
C. Connectivity map							
VS (L) Positive							
Inferior Occipital Gyrus (L)		52		8.1	-21	-91	-5
Inferior Occipital Gyrus (R)		37		7.43	21	-88	-11
VS (L) Negative							
Lingual Gyrus (L/R)		1129		8.53	-9	-73	-2
Calcarine (L/R)							
Cuneus (L/R)							
Precuneus (L/R)							
Putamen (L)		418		8.52	-21	8	1
Caudate (L)							
Insula (L)							
Supplementary Motor Area (L/R)		1156		8.22	6	5	55
Median Cingulate Gyri (L/R)							
Precentral Gyrus (L/R)							
Putamen (R)		354		7.98	21	8	-8
Caudate (R)							
Middle Temporal Gyrus (R)		256		6.81	48	-61	16
Thalamus (R)		37		6.57	9	-19	4

Middle Frontal Gyrus (L)	67	5.87	-36	41	34
Insula (R)	16	5.87	33	-25	13
Insula (R)	26	5.75	51	2	4
Thalamus (L)	30	5.64	-12	-22	10
Postcentral Gyrus (L)	19	5.53	-57	-22	31
Middle Frontal Gyrus (L)	23	5.52	-24	53	7
Middle Frontal Gyrus (R)	25	5.36	33	41	40
Middle Frontal Gyrus (L)	11	5.36	-39	47	19
Precentral Gyrus (R)	30	5.33	24	-25	55
VS (R) Positive					
Inferior Occipital Gyrus (L)	51	8.37	-21	-91	-5
Inferior Occipital Gyrus (R)	51	7.32	21	-88	-11
VS (R) Negative					
Lingual Gyrus (L/R)	2519	9.64	9	-76	-5
Calcarine (L/R)					
Cuneus (L/R)					
Precuneus (L/R)					
Supplementary Motor Area (L/R)					
Precentral Gyrus (L/R)					
Median Cingulate Gyri (L/R)					
Putamen (L)	452	8.64	-18	8	-2
Caudate (L)					
Insula (L)					
Putamen (R)	360	7.71	21	8	-8
Caudate (R)					
Insula (R)					
Middle Temporal Gyrus (R)	179	7.14	54	-58	16
Thalamus (R)	56	7.11	9	-19	4
Thalamus (L)	50	6.77	-9	-22	4
Lingual Gyrus (R)	23	6.38	21	-49	-8
Middle Frontal Gyrus (L)	67	6.15	-33	41	31
Middle Frontal Gyrus (R)	33	5.7	30	38	34
Supramarginal Gyrus (R)	65	5.68	63	-46	22
Precentral Gyrus (R)	55	5.57	24	-34	67
Insula (R)	13	5.41	36	-31	19
Superior Temporal Gyrus (R)	11	5.27	60	-34	13

Mapping adolescent reward anticipation, receipt and prediction error during the Monetary Incentive Delay task

Results

With cluster-wise FWE corrected threshold $p < 0.05$, male adolescents in early pubertal stage (PDS Stage 2) showed more brain activation in calcarine ($t = 4.35$, cluster size: 79, MNI: 27, -61, 10) and superior temporal gyrus ($t = 4.04$, cluster size: 60, MNI: 39, -31, 4) compared with those in late puberty stage (PDS Stage 4) during reward anticipation. Right VS connections with left inferior parietal gyrus ($t = 4.47$, cluster size: 39, MNI: 36, -34, 34) were heightened in males in early pubertal stage compared with late stage. In addition, the comparison of female adolescent group (PDS Stage 5 vs. PDS Stage 3) demonstrated significant difference on connectivity that between left thalamus and left precuneus ($t = 4.50$, cluster size: 55, MNI: -3, -40, 64) during reward receipt.

Tables and Figures

Table S1. Statistical information for regional peak voxels and selected ROIs in the activation maps and probabilistic maps

	Reginal Peak voxel					Selected ROIs				
Reward anticipation	T value	MNI(x,y,z)			Probability	T value	MNI(x,y,z)			Probability
Thalamus (L)	49	-12	-19	10	1.00	47.99	-9	-19	7	1.00
Thalamus (R)	49.37	12	-13	7	1.00	45.5	9	-19	7	1.00
Reward receipt										
vmPFC (L)	25.83	0	38	4	0.97	23.84	-3	41	7	0.90
vmPFC (R)	23.53	3	41	7	0.88	23.53	3	41	7	0.86
Thalamus (L)	29.97	-6	-22	-2	1.00	29.46	-9	-19	7	1.00
Thalamus (R)	28.18	9	-19	10	1.00	30.51	9	-19	7	0.98
Reward PE										
VS (L)	24.11	-12	14	-8	0.89	24.11	-12	14	-8	0.89
VS (R)	25.13	12	14	-8	0.92	25.13	12	14	-8	0.92

Table S2. Regions that showed different activities between male and female adolescents (male > female) during reward anticipation.

Region	**Cluster size (voxels)**	**Peak**	**MNI(x,y,z)**		
Middle Temporal Gyrus (R)	22	6.13	63	-16	-14
Putamen (L)	13	5.81	-30	-13	4
Precuneus (R)	17	5.81	9	-70	40
Inferior Frontal Gyrus, Orbital Part (L)	3	5.54	-48	29	-8
Putamen (R)	28	5.53	30	-7	1
Putamen (L)	6	5.37	-24	2	1
Middle Temporal Gyrus (L)	4	5.37	-60	-19	-11
Precuneus (R)	3	5.31	9	-58	31
Putamen (L)	4	5.25	24	2	-8
Superior Frontal Gyrus (R)	3	5.07	27	32	52
Caudate (R)	2	5.06	12	11	7
Putamen (L)	2	5.05	-27	-4	-8
Angular Gyrus (R)	3	5.00	48	-67	34
Superior Temporal Gyrus (L)	1	4.93	-42	-25	4
Precuneus (L)	1	4.89	-6	-70	40
Inferior Frontal Gyrus, Triangular Part (R)	1	4.81	36	20	28
Inferior Frontal Gyrus, Triangular Part (R)	1	4.73	51	38	-2

Table S3. Regions that showed different activities between male and female adolescents (male > female) in processing of reward PE.

Region	Cluster size (voxels)	Peak	MNI(x,y,z)		
Precuneus (R)	22	6.39	6	-73	40
Middle Temporal Gyrus (R)	10	5.79	57	-19	-14
Putamen (L)	18	5.70	-27	-4	-8
Putamen (L)	20	5.64	-30	-13	4
Superior Temporal Gyrus (L)	13	5.38	-60	-10	10
Caudate (R)	8	5.30	12	11	10
Middle Temporal Gyrus (L)	3	5.23	-60	-46	4
Superior Temporal Gyrus (L)	4	5.21	-45	-28	4
Caudate (L)	6	5.15	-9	8	7
Hippocampus (L)	3	5.06	15	-25	-5
Middle Temporal Gyrus (L)	2	5.05	-57	-22	-11
Postcentral Gyrus (L)	3	5.05	-42	-16	40
Superior Temporal Gyrus (L)	2	5.04	-63	-28	7
Putamen (L)	3	5.01	24	2	-8
Rolandic Operculum (R)	2	4.90	51	-13	10
Putamen (R)	2	4.87	18	11	1
Pallidum (R)	1	4.87	24	-1	4
Precentral Gyrus (R)	1	4.87	54	-7	46
Putamen (R)	1	4.86	18	8	-11
Precuneus (L)	1	4.80	-9	-67	34
Thalamus (L)	2	4.79	-6	-22	10
Postcentral Gyrus (L)	1	4.79	-48	-22	49
Middle Temporal Gyrus (R)	1	4.75	-45	-40	-5
Lingual Gyrus (L)	1	4.75	-6	-85	-5
Putamen (R)	1	4.74	24	14	-5

Table S4. Regions that showed significant changes in functional connectivity with thalamus and VS during reward anticipation. Main regions within the cluster, cluster size, peak t-value within the cluster as well as the corresponding MNI coordinates are shown in the table. (L = left; R = right; L/R=bilateral)

Region	Cluster size (voxels)	Peak	MNI (x,y,z)		
Thalamus (L) Positive					
Lingual Gyrus (L/R)	1208	9.63	9	-88	16
Calcarine (L/R)					
Cuneus (L/R)					
Supplementary Motor Area (L/R)	174	7.16	3	2	64
Dorsal cingulate gyri (L/R)					
Insula (L)	25	5.76	-33	14	10
Insula (L)	13	5.38	-45	2	4
Inferior Frontal Gyrus, Opercular Part (R)	10	5.46	33	23	-8
Putamen (L)	6	5.46	-18	8	1
Middle Temporal Gyrus (R)	5	5.59	45	-76	13
Insula (L)	4	5.02	-33	17	-11
Putamen (R)	4	4.95	21	14	-2
Insula (R)	3	5.06	33	29	4
Superior Temporal Gyrus (R)	2	5.06	51	8	1
Insula (R)	2	5.29	42	17	4
Middle Occipital Gyrus (L)	2	4.9	-27	-79	19
Midbrain (L)	1	4.98	-3	-28	-5
Thalamus (L) Negative					
Inferior Occipital Gyrus (L)	137	15.66	-30	-88	-8
Inferior Occipital Gyrus (R)	165	15.04	21	-88	-11
Postcentral Gyrus (R)	83	6.93	57	-7	28
Postcentral Gyrus (L)	67	6.55	-51	-10	31
Inferior Frontal Gyrus, Opercular Part (L)	26	5.99	-48	17	34
Middle Frontal Gyrus (L)	7	5.05	-24	20	49
Thalamus (R)	3	5.25	21	-28	-2
Precentral Gyrus (R)	2	5.01	60	-7	13
Thalamus (R) Positive					
Lingual Gyrus (L/R)	708	9.02	9	-91	16
Calcarine (L/R)					
Cuneus (L/R)					

Supplementary Motor Area (L/R)	50	6.66	0	2	61
Insula (L)	33	6.23	-33	17	10
Dorsal cingulate gyri (L)	24	5.66	-6	14	37
Putamen (R)	16	5.57	21	11	1
Insula (R)	11	5.73	48	5	1
Calcarine (R)	10	5.07	24	-64	13
Inferior Frontal Gyrus, Orbital Part (R)	6	5.44	30	23	-11
Precentral Gyrus (R)	6	5.17	42	-13	55
Lingual Gyrus (R)	3	5.12	24	-49	-8
Insula (L)	3	5.09	-33	17	-8
Inferior Frontal Gyrus, Opercular Part (R)	2	4.95	45	14	4
Supplementary Motor Area (R)	2	4.83	6	-7	52
Parahippocampal Gyrus (R)	1	5.13	18	-40	-5
Pallidum (L)	1	5.09	-9	5	-2
Putamen (L)	1	4.84	-15	8	1
Lingual Gyrus (L)	1	4.75	-18	-55	-2
Insula (L)	1	4.74	30	29	4
Thalamus (R) Negative					
Inferior Occipital Gyrus (L)	195	16.76	-27	-88	-8
Inferior Occipital Gyrus (R)	171	15.18	33	-85	-8
Postcentral Gyrus (L)	119	7.91	-57	-10	34
Postcentral Gyrus (R)	108	7.3	60	-7	28
Middle Frontal Gyrus (L)	73	6.25	-42	14	31
Angular Gyrus (R)	67	6.14	39	-70	40
Precuneus (R)	31	6.01	6	-61	49
Postcentral Gyrus (L)	23	5.99	-36	-31	67
Angular Gyrus (L)	68	5.72	-33	-67	37
Middle Frontal Gyrus (L)	15	5.36	-33	17	55
Middle Frontal Gyrus (R)	8	5.25	45	35	19
Superior Parietal Gyrus (L)	5	5.55	-30	-46	67
Rolandic Operculum (L)	4	5.25	-39	-13	19
Middle Frontal Gyrus (R)	3	5.08	30	20	58
Middle Frontal Gyrus (L)	2	5.12	-24	23	43
Rolandic Operculum (R)	1	5.36	60	-10	10
Middle Frontal Gyrus (L)	1	4.97	-45	26	40
Thalamus (R)	1	4.88	21	-28	-2
Precentral Gyrus (L)	1	4.73	-33	-19	67
VS (L) Positive					
Lingual Gyrus (L/R)	1375	9.78	9	-88	22

Calcarine (L/R)					
Cuneus (L/R)					
Supplementary Motor Area (L/R)	612	9.77	3	5	61
Median Cingulate Gyri (L/R)					
Precentral Gyrus (R)	84	8.02	45	-7	52
Insula (L)	40	7.67	-30	20	10
Precentral Gyrus (L)	84	7.37	-42	-7	55
Putamen (R)	85	7.33	21	14	-2
Median Cingulate Gyri (L)	38	6.84	-12	-22	40
Insula (L)	48	6.55	-45	11	1
Thalamus (R)	43	6.16	6	-13	-2
Putamen (L)	26	5.44	-21	14	-2
Thalamus (L)	16	6.05	-6	-22	4
Superior Temporal Gyrus (L)	11	5.66	51	11	-2
Supplementary Motor Area (R)	8	4.98	6	-22	49
Thalamus (R)	7	5.67	-6	-16	-8
Putamen (L)	5	5.33	-24	5	4
Superior Parietal Gyrus (L)	3	5.05	-27	-52	58
Cerebellum (L)	2	5.90	-33	-55	-32
Cerebellum (R)	2	5.45	33	-52	-32
Precentral Gyrus (L)	2	4.98	-51	-1	43
Putamen (L)	1	4.87	-21	5	-11
Calcarine (R)	1	4.85	24	-58	13
VS (L) Negative					
Inferior Occipital Gyrus (L)	103	15.26	-21	-91	-5
Inferior Occipital Gyrus (R)	104	13.72	33	-85	-8
Angular Gyrus (L)	67	7.16	-42	-73	37
Postcentral Gyrus (L)	45	7.14	-54	-7	28
Postcentral Gyrus (R)	83	6.99	57	-7	28
Inferior Frontal Gyrus, Triangular Part (R)	54	6.56	48	38	16
Inferior Frontal Gyrus, Opercular Part (L)	51	6.52	-45	17	34
Middle Frontal Gyrus (L)	59	6.40	-30	23	55
Superior Frontal Gyrus, Medial Orbital (R)	41	5.99	6	47	-11
Superior Frontal Gyrus (R)	37	5.86	30	26	55
Inferior Frontal Gyrus, Triangular Part (L)	31	5.71	-45	35	10

Angular Gyrus (R)	19	6.02	45	-67	40
Superior Temporal Gyrus (R)	17	5.77	57	-10	4
Inferior Frontal Gyrus, Triangular Part (L)	12	5.36	-54	26	7
Anterior Cingulate Gyri (L)	11	4.98	-6	38	1
Superior Frontal Gyrus (L)	4	5.56	-21	62	7
Superior Frontal Gyrus (L)	4	5.25	-9	56	37
Precuneus (L)	3	5.07	0	-61	25
Inferior Frontal Gyrus, Orbital Part (R)	2	5.19	36	32	-11
Olfactory Cortex (L)	2	5.16	0	17	-5
Superior Frontal Gyrus, Medial Orbital (R)	2	5.06	9	41	-2
Anterior Cingulate Gyri (L)	2	5.01	-9	32	-11
Caudate (L)	2	5.01	24	-4	28
Precuneus (L)	1	4.83	-9	-58	43
Hippocampus (R)	1	4.82	27	-4	-23
Anterior Cingulate Gyri (R)	1	4.80	6	35	-8
Precuneus (L)	1	4.79	-6	-46	40
Superior Frontal Gyrus (L)	1	4.74	-21	53	1
Rolandic Operculum (R)	1	4.72	54	-19	10
VS (R) Positive					
Supplementary Motor Area (L/R)	884	10.44	0	-1	61
Median Cingulate Gyri (L/R)					
Lingual Gyrus (L/R)	1595	10.41	9	-88	22
Calcarine (L/R)					
Cuneus (L/R)					
Precentral Gyrus (R)	122	8.16	42	-10	55
Insula (L)	119	7.85	-33	20	10
Thalamus (L)	58	7.36	-6	-22	7
Precentral Gyrus (L)	78	6.98	-36	-7	46
Thalamus (R)	89	6.66	6	-16	1
Insula (R)	61	6.42	33	26	7
Putamen (R)	73	6.30	21	11	-2
Putamen (L)	57	6.09	-12	8	-2
Precentral Gyrus (L)	13	6.45	-51	-1	43
Inferior Parietal Gyrus (L)	11	5.46	-24	-52	52
Inferior Frontal Gyrus, Orbital Part (R)	8	5.61	33	23	-8
Cerebelum (R)	6	5.70	36	-52	-32
Putamen (L)	5	4.97	-24	8	7
Cerebelum (L)	4	6.14	-33	-55	-32
Superior Occipital Gyrus (L)	4	5.00	-15	-67	37
Supplementary Motor Area (L)	1	4.86	-6	-19	52

Supramarginal Gyrus (R)	1	4.86	57	-46	28
Cerebelum (L)	1	4.80	-27	-61	-23
Caudate (L)	1	4.75	3	-1	7
VS (R) Negative					
Inferior Occipital Gyrus (L)	107	14.61	-30	-88	-8
Inferior Occipital Gyrus (R)	98	14.51	33	-85	-8
Angular Gyrus (L)	38	7.33	-42	-73	34
Postcentral Gyrus (R)	45	6.54	57	-7	31
Angular Gyrus (R)	28	6.08	48	-67	37
Postcentral Gyrus (L)	21	5.66	-54	-10	31
Superior Temporal Gyrus (R)	18	5.96	60	-7	4
Superior Frontal Gyrus, Medial Orbital (R)	18	5.68	9	50	-11
Inferior Frontal Gyrus, Triangular Part (L)	15	5.30	-45	38	-2
Middle Frontal Gyrus (L)	14	5.31	-30	23	55
Inferior Frontal Gyrus, Opercular Part (L)	13	5.61	-39	17	31
Middle Frontal Gyrus (R)	11	5.68	30	20	58
Olfactory Cortex (L)	5	5.68	0	17	-8
Precuneus (L)	5	5.46	0	-61	25
Anterior Cingulate Gyri (R)	3	5.08	9	35	-8
Superior Frontal Gyrus (L)	3	4.95	-24	53	1
Inferior Frontal Gyrus, Triangular Part (L)	2	4.91	-51	26	1
Superior Temporal Gyrus (L)	2	4.79	-60	-22	7
Superior Frontal Gyrus (L)	1	5.17	-9	56	37
Inferior Frontal Gyrus, Triangular Part (R)	1	4.96	51	35	13
Hippocampus (R)	1	4.82	27	-4	-23
Postcentral Gyrus (L)	1	4.78	-48	-13	34

Table S5. Regions that showed significant changes in functional connectivity with vmPFC during reward receipt.

Region	Cluster size (voxels)	Peak	MNI (x,y,z)		
vmPFC (L) Positive					
Middle Occipital Gyrus (L)	302	18.48	-27	-88	-11
Inferior Occipital Gyrus (L)					
Middle Occipital Gyrus (R)	302	18.44	21	-88	-11
Inferior Occipital Gyrus (R)					
Angular Gyrus (R)	94	6.86	30	-70	28
Inferior Frontal Gyrus, Triangular Part (R)	24	6.02	54	23	22
Median Cingulate Gyri (R)	19	5.58	3	-22	31
Hippocampus (L)	12	7.15	24	-28	-2

Inferior Frontal Gyrus, Opercular Part (R)	12	5.22	51	14	34
Thalamus (R)	9	6.59	-18	-31	-2
Middle Occipital Gyrus (L)	6	5.63	-27	-73	28
Fusiform Gyrus (R)	5	5.69	33	-52	-17
Inferior Parietal Gyrus (R)	3	4.97	51	-43	52
Middle Frontal Gyrus (R)	2	4.97	45	14	49
Inferior Frontal Gyrus, Orbital Part (R)	1	4.89	42	26	-11
Inferior Frontal Gyrus, Orbital Part (R)	1	4.86	45	23	-8
Cerebelum (R)	1	4.83	33	-46	-23
vmPFC (L) Negative					
Cuneus (L/R)	674	9.94	-9	-76	-5
Calcarine (L/R)					
Lingual Gyrus (L/R)					
Supplementary Motor Area (L)	299	8.91	-6	2	58
Insula (L)	153	6.83	-21	8	10
Dorsal striatum (L)					
Precentral Gyrus (L)	103	6.67	-42	-10	49
Undefined	31	5.99	3	5	16
Precuneus (L)	23	5.98	-9	-58	61
Calcarine (R)	27	5.62	33	-55	1
Middle Frontal Gyrus (R)	20	6.26	39	-7	52
Insula (R)	19	6.83	36	14	7
Thalamus (R)	17	5.71	-15	-28	22
Putamen (R)	12	5.33	24	8	7
Lingual Gyrus (R)	11	5.54	18	-46	-8
Superior Parietal Gyrus (R)	10	5.19	18	-58	61
Middle Frontal Gyrus (L)	5	5.19	-33	41	28
Precuneus (R)	4	4.97	12	-52	58
Lingual Gyrus (R)	3	5.57	27	-73	1
Lingual Gyrus (R)	3	5.26	18	-58	-8
Precuneus (L)	1	5.06	21	-43	13
Thalamus (R)	1	4.83	-6	-19	-5
Posterior Cingulate Gyrus (L)	1	4.80	18	-40	16
Superior Frontal Gyrus (L)	1	4.78	-24	53	7
vmPFC (R) Positive					
Middle Occipital Gyrus (L)	265	18.3	-27	-88	-11
Inferior Occipital Gyrus (L)					
Middle Occipital Gyrus (R)	278	17.67	21	-88	-11
Inferior Occipital Gyrus (R)					

Middle Occipital Gyrus (R)	51	6.64	30	-70	28
Hippocampus (L)	6	6.78	24	-28	-2
Inferior Frontal Gyrus, Triangular Part (R)	4	5.63	54	23	22
Thalamus (R)	3	5.33	-21	-28	-2
Fusiform Gyrus (R)	2	5.45	33	-52	-17
Cerebellum (R)	1	4.84	33	-46	-23
Median Cingulate Gyri (R)	1	4.76	3	-28	28
vmPFC (R) Negative					
Cuneus (L/R)	852	10.04	-6	-79	-5
Calcarine (L/R)					
Lingual Gyrus (L/R)					
Supplementary Motor Area (L/R)	522	9.2	-6	5	55
Precentral Gyrus (L)					
Precuneus (L)	80	7.24	-9	-58	61
Precentral Gyrus (R)	61	7.12	42	-4	52
Insula (L)	54	6.38	-39	11	7
Middle Frontal Gyrus (L)	29	6.3	-33	38	31
Precuneus (R)	44	6.24	9	-52	58
Dorsal striatum (L)	29	6.13	-21	8	10
Middle Frontal Gyrus (R)	22	5.64	30	35	31
Caudate (L)	15	5.82	3	8	13
Insula (R)	10	5.78	36	14	7
Thalamus (L)	9	5.55	-6	-16	-2
Fusiform Gyrus (R)	8	5.12	-33	-49	-2
Median Cingulate Gyri (L)	5	5.31	-15	-37	43
Median Cingulate Gyri (R)	3	5.34	-12	-16	37
Posterior Cingulate Gyrus (R)	3	4.93	-15	-40	16
Pallidum (R)	3	4.89	21	5	-2
Cerebellum (R)	2	5.30	0	-46	-17
Superior Parietal Gyrus (L)	2	5.05	-24	-55	64
Insula (L)	2	5.03	24	35	7
Rolandic Operculum (R)	2	4.94	57	5	13
Thalamus (R)	2	4.92	-18	-31	19
Median Cingulate Gyri (R)	1	5.08	12	-7	40
Thalamus (R)	1	5.06	6	-22	1
Precentral Gyrus (L)	1	4.94	-57	2	22
Calcarine (L)	1	4.74	-24	-58	10

Table S6. Regions that showed significant changes in functional connectivity with thalamus during reward receipt.

Region	Cluster size (voxels)	Peak	MNI (x,y,z)		
Thalamus (L) Negative					
Inferior Occipital Gyrus (L)	214	10.77	-30	-88	-8
Inferior Occipital Gyrus (R)	260	10.36	21	-88	-11
Superior Temporal Gyrus (R)	869	9.31	48	-13	16
Insula (R)					
Rolandic Operculum (R)					
Postcentral Gyrus (R)					
Superior Temporal Gyrus (L)	1619	9.09	0	-25	13
Rolandic Operculum (L)					
Inferior Frontal Gyrus, Triangular Part (L)					
Insula (L)					
Postcentral Gyrus (L)					
Angular Gyrus (L)	103	7.89	-48	-67	34
Superior Frontal Gyrus (L/R)	536	7.65	-18	35	46
Superior Frontal Gyrus, Medial (L/R)					
Middle Frontal Gyrus (L)					
Cerebellum (L)	30	6.86	-3	-43	-26
Cerebellum (R)	33	6.84	24	-34	-26
Postcentral Gyrus (L)	61	6.51	-30	-40	61
Precuneus (L)	70	6.42	-3	-55	7
Middle Frontal Gyrus (R)	23	6.28	36	23	49
Postcentral Gyrus (R)	26	6.26	24	-40	67
Inferior Frontal Gyrus, Triangular Part (R)	83	6.26	48	41	19
Superior Frontal Gyrus (R)	43	6.05	12	41	52
Postcentral Gyrus (R)	65	5.94	42	-34	61
Angular Gyrus (R)	44	5.89	36	-73	37
Insula (R)	22	5.88	21	29	13
Median Cingulate Gyri (L/R)	40	5.67	6	-4	37
Thalamus (R)	18	5.88	18	-31	-2
Middle Temporal Gyrus (R)	16	5.98	60	-10	-14

Cerebellum (L)	15	6.39	-27	-37	-29
Thalamus (R)	13	5.76	24	-28	16
Caudate (L)	13	5.47	18	11	22
Hippocampus (L)	13	5.45	-33	-37	-5
Precuneus (R)	9	5.31	12	-46	67
Caudate (L)	8	5.51	6	26	7
Inferior Frontal Gyrus, Orbital Part (R)	6	5.81	30	38	-8
Cerebellum (L)	6	5.23	-30	-52	-23
Postcentral Gyrus (L)	5	5.35	-51	-37	55
Superior Frontal Gyrus, Medial (L)	5	5.24	-3	59	28
Calcarine (R)	5	5.20	-27	-49	7
Inferior Frontal Gyrus, Triangular Part (L)	5	5.18	-39	29	19
Lingual Gyrus (L)	4	5.60	-12	-34	-2
Caudate (R)	4	5.55	-21	32	10
Inferior Temporal Gyrus (R)	4	5.22	48	-49	-17
Putamen (R)	4	5.08	30	-1	-11
Median Cingulate Gyri (R)	4	4.99	3	-13	49
Precentral Gyrus (R)	4	4.97	45	-19	61
Postcentral Gyrus (R)	4	4.97	27	-37	55
Angular Gyrus (R)	4	4.90	39	-64	46
Hippocampus (R)	3	5.36	-39	-22	-14
Superior Temporal Gyrus (L)	3	5.27	-60	-46	16
Hippocampus (R)	3	5.23	24	-16	-17
Supramarginal Gyrus (L)	3	5.07	-57	-25	40
Temporal Pole: Superior Temporal Gyrus (R)	2	5.17	39	17	-26
Inferior Parietal Gyrus (L)	2	5.12	-48	-61	46
Precuneus (L)	2	5.08	-6	-46	40
Paracentral Lobule (R)	2	5.01	15	-34	55
Precentral Gyrus (R)	2	4.97	36	-22	67
Hippocampus (R)	2	4.96	39	-22	-14
Superior Frontal Gyrus, Medial (L)	2	4.96	-3	35	46
Hippocampus (L)	2	4.90	-24	-13	-14
Hippocampus (R)	2	4.83	39	-34	-11
Middle Frontal Gyrus (R)	2	4.79	42	53	7
Postcentral Gyrus (R)	2	4.77	-24	-31	31
Inferior Frontal Gyrus, Orbital Part (R)	1	5.23	36	35	-11
Precentral Gyrus (L)	1	5.15	18	-19	55
Lingual Gyrus (R)	1	5.04	-6	-43	4
Postcentral Gyrus (R)	1	4.94	60	-1	34
Postcentral Gyrus (L)	1	4.90	-48	-22	40
Hippocampus (L)	1	4.88	15	-13	-14
Superior Frontal Gyrus (R)	1	4.87	27	-10	67
Inferior Parietal Gyrus (L)	1	4.87	-51	-49	40
Middle Temporal Gyrus (L)	1	4.86	-54	-46	-2
Superior Parietal Gyrus (R)	1	4.82	18	-55	67

Precuneus (L)	1	4.80	-6	-58	34
Middle Frontal Gyrus (R)	1	4.79	30	17	40
Superior Frontal Gyrus (L)	1	4.79	-12	65	16
Middle Frontal Gyrus (R)	1	4.78	24	26	43
Inferior Temporal Gyrus (L)	1	4.78	-48	-55	-17
Superior Parietal Gyrus (R)	1	4.76	24	-52	64
Anterior Cingulate Gyri (L)	1	4.76	3	-7	28
Cerebellum (R)	1	4.76	27	-55	-20
Postcentral Gyrus (L)	1	4.75	-42	-34	64
Inferior Frontal Gyrus, Opercular Part (R)	1	4.75	48	11	19
Cerebellum (R)	1	4.75	33	-64	-23
Hippocampus (L)	1	4.74	24	-16	-11
Median Cingulate Gyri (R)	1	4.74	3	-19	34
Fusiform Gyrus (L)	1	4.73	-42	-58	-17
Thalamus (R) Negative					
Inferior Occipital Gyrus (L)	118	10.42	-30	-88	-8
Inferior Occipital Gyrus (R)	195	9.32	21	-88	-11
Superior Temporal Gyrus (R)	377	8.03	54	-28	16
Insula (R)					
Superior Temporal Gyrus (L)	519	6.84	-54	-7	4
Inferior Frontal Gyrus, Triangular Part (L)					
Insula (L)					
Undefined	58	6.35	6	2	16
Cerebelum (R)	25	6.31	27	-34	-26
Inferior Frontal Gyrus, Triangular Part (R)	64	6.02	51	38	16
Superior Frontal Gyrus (L)	23	5.31	-15	38	46
Median Cingulate Gyri (L)	19	5.66	0	-4	37
Middle Temporal Gyrus (R)	15	5.40	66	-37	1
Angular Gyrus (L)	11	5.74	-48	-67	34
Inferior Parietal Gyrus (R)	10	5.47	54	-31	55
Cerebellum (R)	9	5.19	0	-46	-29
Middle Temporal Gyrus (R)	8	5.55	60	-10	-14
Supramarginal Gyrus (R)	8	5.55	60	-25	43
Postcentral Gyrus (L)	8	5.16	-30	-40	58
Precentral Gyrus (L)	8	5.12	-48	11	34
Thalamus (L)	7	6.31	0	-25	13
Postcentral Gyrus (R)	7	5.78	63	-13	34
Middle Temporal Gyrus (L)	7	5.29	-63	-37	-8

Superior Frontal Gyrus, Medial Orbital (L)	7	5.11	-6	53	-5
Hippocampus (R)	5	5.31	18	-31	-5
Middle Temporal Gyrus (L)	5	5.23	-54	-34	-8
Middle Temporal Gyrus (L)	5	5.16	-63	-19	-11
Precuneus (R)	5	5.12	9	-49	7
Inferior Frontal Gyrus, Triangular Part (L)	5	5.02	-48	23	25
Postcentral Gyrus (L)	5	4.94	-48	-19	37
Postcentral Gyrus (L)	4	5.05	-57	-13	19
Superior Temporal Gyrus (R)	4	4.93	63	-28	4
Middle Temporal Gyrus (L)	3	5.21	-51	-70	16
Middle Frontal Gyrus (L)	2	5.22	-21	29	55
Hippocampus (L)	2	5.20	-36	-22	-14
Amygdala (R)	2	5.20	-27	-4	-11
Inferior Temporal Gyrus (L)	2	5.19	-54	-64	-8
Cerebellum (R)	2	5.18	-27	-37	-29
Angular Gyrus (R)	2	5.15	42	-61	28
Postcentral Gyrus (L)	2	5.15	-21	-43	67
Postcentral Gyrus (R)	2	5.09	48	-22	40
Postcentral Gyrus (R)	2	4.92	63	-7	22
Insula (R)	1	5.12	36	-22	13
Middle Temporal Gyrus (R)	1	5.11	60	-46	-8
Anterior Cingulate Gyri (L)	1	5.08	-12	47	-5
Superior Frontal Gyrus, Medial Orbital (R)	1	5.04	6	53	-11
Middle Temporal Gyrus (L)	1	4.99	-57	-52	4
Superior Frontal Gyrus (R)	1	4.91	21	44	46
Inferior Frontal Gyrus, Orbital Part (L)	1	4.86	-48	41	-5
Fusiform Gyrus (R)	1	4.85	33	-37	-17
Inferior Temporal Gyrus (L)	1	4.85	45	-40	-14
Postcentral Gyrus (L)	1	4.83	-54	-19	40
Fusiform Gyrus (L)	1	4.82	-24	-40	-14
Hippocampus (R)	1	4.81	24	-4	-20
Superior Frontal Gyrus, Medial (L)	1	4.81	-9	41	49
Postcentral Gyrus (L)	1	4.80	-57	-16	43
Middle Temporal Gyrus (L)	1	4.80	-54	-13	-11
Thalamus (L)	1	4.78	-3	-16	16
Anterior Cingulate Gyri (L)	1	4.75	-3	44	1
Middle Temporal Gyrus (R)	1	4.75	54	-4	-17

Table S7. Regions that showed significant changes in functional connectivity with VS during reward PE.

Region	**Cluster size (voxels)**	**Peak**	**MNI (x,y,z)**
VS (L) Negative			

Inferior Occipital Gyrus (L)	52	8.1	-21	-91	-5
Inferior Occipital Gyrus (R)	37	7.43	21	-88	-11
Middle Occipital Gyrus (R)	1	5.65	24	-88	7
VS (L) Positive					
Lingual Gyrus (L/R)	1129	8.53	-9	-73	-2
Calcarine (L/R)					
Cuneus (L/R)					
Precuneus (L/R)					
Putamen (L)	418	8.52	-21	8	1
Caudate (L)					
Insula (L)					
Supplementary Motor Area (L/R)	1156	8.22	6	5	55
Median Cingulate Gyri (L/R)					
Precentral Gyrus (L/R)					
Putamen (R)	354	7.98	21	8	-8
Caudate (R)					
Middle Temporal Gyrus (R)	256	6.81	48	-61	16
Thalamus (R)	37	6.57	9	-19	4
Middle Frontal Gyrus (L)	67	5.87	-36	41	34
Insula (R)	26	5.75	51	2	4
Thalamus (L)	30	5.64	-12	-22	10
Middle Frontal Gyrus (L)	23	5.52	-24	53	7
Middle Frontal Gyrus (R)	25	5.36	33	41	40
Precentral Gyrus (R)	30	5.33	24	-25	55
Postcentral Gyrus (L)	19	5.53	-57	-22	31
Insula (R)	16	5.87	33	-25	13
Middle Frontal Gyrus (L)	11	5.36	-39	47	19
Cerebellum (R)	9	5.32	6	-46	-14
Superior Temporal Gyrus (R)	8	5.26	63	-34	16
Middle Temporal Gyrus (L)	8	5.26	-54	-64	19
Hippocampus (L)	6	5.29	24	-40	16
Precentral Gyrus (L)	5	5.38	-51	-1	40
Caudate (L)	5	5.07	15	-28	22
Middle Occipital Gyrus (L)	5	5.04	-39	-79	19
Insula (L)	4	5.36	-30	26	1
Paracentral Lobule (R)	4	5.13	9	-37	58

Thalamus (L)	3	5.40	6	-13	-5
Angular Gyrus (R)	3	5.22	51	-49	31
Middle Occipital Gyrus (R)	3	5.05	45	-76	22
Lingual Gyrus (L)	3	5.03	-24	-55	-8
Precentral Gyrus (L)	3	5.01	-30	-25	52
Parahippocampal Gyrus (R)	3	4.87	24	-43	-11
Insula (L)	2	4.87	-27	20	10
Inferior Parietal Gyrus (L)	1	5.11	-60	-43	37
Superior Temporal Gyrus (R)	1	5.10	63	-16	1
Inferior Parietal Gyrus (L)	1	4.95	-57	-46	40
Lingual Gyrus (R)	1	4.90	21	-52	-11
Middle Occipital Gyrus (L)	1	4.88	39	-67	7
Superior Temporal Gyrus (R)	1	4.87	63	-10	1
Precentral Gyrus (R)	1	4.80	54	5	40
Postcentral Gyrus (L)	1	4.79	-24	-37	61
Paracentral Lobule (R)	1	4.75	3	-31	64
VS (R) Negative					
Inferior Occipital Gyrus (L)	51	8.37	-21	-91	-5
Inferior Occipital Gyrus (R)	51	7.32	21	-88	-11
Inferior Occipital Gyrus (L)	2	4.86	-39	-76	-11
Middle Occipital Gyrus (R)	1	5.30	24	-88	7
VS (R) Positive					
Lingual Gyrus (L/R)	2519	9.64	9	-76	-5
Calcarine (L/R)					
Cuneus (L/R)					
Precuneus (L/R)					
Supplementary Motor Area (L/R)					
Precentral Gyrus (L/R)					
Median Cingulate Gyri (L/R)					
Putamen (L)	452	8.64	-18	8	-2
Caudate (L)					
Insula (L)					
Putamen (R)	360	7.71	21	8	-8
Caudate (R)					
Insula (R)					
Middle Temporal Gyrus (R)	179	7.14	54	-58	16
Thalamus (R)	56	7.11	9	-19	4

Thalamus (L)	50	6.77	-9	-22	4
Lingual Gyrus (R)	23	6.38	21	-49	-8
Middle Frontal Gyrus (L)	67	6.15	-33	41	31
Middle Frontal Gyrus (R)	33	5.7	30	38	34
Supramarginal Gyrus (R)	65	5.68	63	-46	22
Precentral Gyrus (R)	55	5.57	24	-34	67
Supramarginal Gyrus (L)	21	5.90	-54	-28	28
Insula (R)	13	5.41	36	-31	19
Superior Temporal Gyrus (R)	11	5.27	60	-34	13
Insula (L)	7	5.78	-30	26	10
Middle Temporal Gyrus (L)	7	5.07	39	-49	16
Putamen (L)	5	5.12	27	-13	10
Median Cingulate Gyri (R)	5	5.08	-12	-16	37
Postcentral Gyrus (L)	4	5.10	-33	-43	58
Paracentral Lobule (R)	4	4.99	6	-37	52
Insula (L)	2	5.00	-36	-13	-2
Median Cingulate Gyri (R)	2	4.90	-18	-34	40
Postcentral Gyrus (R)	2	4.89	12	-40	67
Inferior Parietal Gyrus (L)	2	4.87	-48	-25	40
Middle Temporal Gyrus (R)	2	4.79	-39	-61	13
Median Cingulate Gyri (R)	2	4.77	15	-25	40
Inferior Frontal Gyrus, Triangular Part (L)	1	4.95	33	23	19
Insula (R)	1	4.87	36	-16	1
Median Cingulate Gyri (R)	1	4.87	12	-19	40
Heschl Gyrus (R)	1	4.86	45	-19	4
Putamen (R)	1	4.85	33	-19	4
Inferior Frontal Gyrus, Orbital Part (L)	1	4.83	-21	35	-11
Middle Temporal Gyrus (L)	1	4.82	-45	-49	22
Supramarginal Gyrus (L)	1	4.81	-60	-25	37
Caudate (R)	1	4.80	18	17	13
Superior Temporal Gyrus (R)	1	4.79	54	-37	19
Postcentral Gyrus (R)	1	4.78	33	-34	43
Supramarginal Gyrus (L)	1	4.77	-60	-40	34
Rolandic Operculum (L)	1	4.75	-39	-4	16
Superior Parietal Gyrus (L)	1	4.75	-24	-52	55
Supramarginal Gyrus (L)	1	4.75	-57	-31	40

Table S8. MNI coordinates used for the connectivity plots

Regions	Abbreviation	MNI(x,y,z)		
Precentral Gyrus (L)	PreCG.L	-38.65	-5.68	50.94
Precentral Gyrus (R)	PreCG.R	41.37	-8.21	52.09

Superior Frontal Gyrus (L)	SFGdor.L	-18.45	34.81	42.2
Superior Frontal Gyrus (R)	SFGdor.R	21.9	31.12	43.82
Superior Frontal Gyrus, Orbital Part (L)	ORBsup.L	-16.56	47.32	-13.31
Superior Frontal Gyrus, Orbital Part (R)	ORBsup.R	18.49	48.1	-14.02
Middle Frontal Gyrus (L)	MFG.L	-33.43	32.73	35.46
Middle Frontal Gyrus (R)	MFG.R	37.59	33.06	34.04
Middle Frontal Gyrus, Orbital Part (L)	ORBmid.L	-30.65	50.43	-9.62
Middle Frontal Gyrus, Orbital Part (R)	ORBmid.R	33.18	52.59	-10.73
Inferior Frontal Gyrus, Opercular Part (L)	IFGoperc.L	-48.43	12.73	19.02
Inferior Frontal Gyrus, Opercular Part (R)	IFGoperc.R	50.2	14.98	21.41
Inferior Frontal Gyrus, Triangular Part (L)	IFGtriang.L	-45.58	29.91	13.99
Inferior Frontal Gyrus, Triangular Part (R)	IFGtriang.R	50.33	30.16	14.17
Inferior Frontal Gyrus, Orbital Part (L)	ORBinf.L	-35.98	30.71	-12.11
Inferior Frontal Gyrus, Orbital Part (R)	ORBinf.R	41.22	32.23	-11.91
Rolandic Operculum (L)	ROL.L	-47.16	-8.48	13.95
Rolandic Operculum (R)	ROL.R	52.65	-6.25	14.63
Supplementary Motor Area (L)	SMA.L	-5.32	4.85	61.38
Supplementary Motor Area (R)	SMA.R	8.62	0.17	61.85
Olfactory Cortex (L)	OLF.L	-8.06	15.05	-11.46
Olfactory Cortex (R)	OLF.R	10.43	15.91	-11.26
Superior Frontal Gyrus, Medial (L)	SFGmed.L	-4.8	49.17	30.89
Superior Frontal Gyrus, Medial (R)	SFGmed.R	9.1	50.84	30.22
Superior Frontal Gyrus, Medial Orbital (L)	ORBsupmed.L	-5.17	54.06	-7.4
Superior Frontal Gyrus, Medial Orbital (R)	ORBsupmed.R	8.16	51.67	-7.13
Gyrus Rectus (L)	REC.L	-5.08	37.07	-18.14
Gyrus Rectus (R)	REC.R	8.35	35.64	-18.04
Insula (L)	INS.L	-35.13	6.65	3.44
Insula (R)	INS.R	39.02	6.25	2.08
Anterior Cingulate Gyri (L)	ACG.L	-4.04	35.4	13.95
Anterior Cingulate Gyri (R)	ACG.R	8.46	37.01	15.84
Median Cingulate Gyri (L)	DCG.L	-5.48	-14.92	41.57
Median Cingulate Gyri (R)	DCG.R	8.02	-8.83	39.79
Posterior Cingulate Gyrus (L)	PCG.L	-4.85	-42.92	24.67
Posterior Cingulate Gyrus (R)	PCG.R	7.44	-41.81	21.87
Hippocampus (L)	HIP.L	-25.03	-20.74	-10.13
Hippocampus (R)	HIP.R	29.23	-19.78	-10.33
Parahippocampal Gyrus (L)	PHG.L	-21.17	-15.95	-20.7
Parahippocampal Gyrus (R)	PHG.R	25.38	-15.15	-20.47
Amygdala (L)	AMYG.L	-23.27	-0.67	-17.14
Amygdala (R)	AMYG.R	27.32	0.64	-17.5
Calcarine (L)	CAL.L	-7.14	-78.67	6.44
Calcarine (R)	CAL.R	15.99	-73.15	9.40
Cuneus (L)	CUN.L	-5.93	-80.13	27.22
Cuneus (R)	CUN.R	13.51	-79.36	28.23
Lingual Gyrus (L)	LING.L	-14.62	-67.56	-4.63
Lingual Gyrus (R)	LING.R	16.29	-66.93	-3.87

Superior Occipital Gyrus (L)	SOG.L	-16.54	-84.26	28.17
Superior Occipital Gyrus (R)	SOG.R	24.29	-80.85	30.59
Middle Occipital Gyrus (L)	MOG.L	-32.39	-80.73	16.11
Middle Occipital Gyrus (R)	MOG.R	37.39	-79.7	19.42
Inferior Occipital Gyrus (L)	IOG.L	-36.36	-78.29	-7.84
Inferior Occipital Gyrus (R)	IOG.R	38.16	-81.99	-7.61
Fusiform Gyrus (L)	FFG.L	-31.16	-40.30	-20.23
Fusiform Gyrus (R)	FFG.R	33.97	-39.1	-20.18
Postcentral Gyrus (L)	PoCG.L	-42.46	-22.63	48.92
Postcentral Gyrus (R)	PoCG.R	41.43	-25.49	52.55
Superior Parietal Gyrus (L)	SPG.L	-23.45	-59.56	58.96
Superior Parietal Gyrus (R)	SPG.R	26.11	-59.18	62.06
Inferior Parietal Gyrus (L)	IPL.L	-42.8	-45.82	46.74
Inferior Parietal Gyrus (R)	IPL.R	46.46	-46.29	49.54
Supramarginal Gyrus (L)	SMG.L	-55.79	-33.64	30.45
Supramarginal Gyrus (R)	SMG.R	57.61	-31.50	34.48
Angular Gyrus (L)	ANG.L	-44.14	-60.82	35.59
Angular Gyrus (R)	ANG.R	45.51	-59.98	38.63
Precuneus (L)	PCUN.L	-7.24	-56.07	48.01
Precuneus (R)	PCUN.R	9.98	-56.05	43.77
Paracentral Lobule (L)	PCL.L	-7.63	-25.36	70.07
Paracentral Lobule (R)	PCL.R	7.48	-31.59	68.09
Caudate (L)	CAU.L	-11.46	11.00	9.24
Caudate (R)	CAU.R	14.84	12.07	9.42
Putamen (L)	PUT.L	-23.91	3.86	2.40
Putamen (R)	PUT.R	27.78	4.91	2.46
Pallidum (L)	PAL.L	-17.75	-0.03	0.21
Pallidum (R)	PAL.R	21.2	0.18	0.23
Thalamus (L)	THA.L	-10.85	-17.56	7.98
Thalamus (R)	THA.R	13	-17.55	8.09
Heschl Gyrus (L)	HES.L	-41.99	-18.88	9.98
Heschl Gyrus (R)	HES.R	45.86	-17.15	10.41
Superior Temporal Gyrus (L)	STG.L	-53.16	-20.68	7.13
Superior Temporal Gyrus (R)	STG.R	58.15	-21.78	6.80
Temporal Pole: Superior Temporal Gyrus (L)	TPOsup.L	-39.88	15.14	-20.18
Temporal Pole: Superior Temporal Gyrus (R)	TPOsup.R	48.25	14.75	-16.86
Middle Temporal Gyrus (L)	MTG.L	-55.52	-33.80	-2.20
Middle Temporal Gyrus (R)	MTG.R	57.47	-37.23	-1.47
Temporal Pole: Middle Temporal Gyrus (L)	TPOmid.L	-36.32	14.59	-34.08
Temporal Pole: Middle Temporal Gyrus (R)	TPOmid.R	44.22	14.55	-32.23
Inferior Temporal Gyrus (L)	ITG.L	-49.77	-28.05	-23.17
Inferior Temporal Gyrus (R)	ITG.R	53.69	-31.07	-22.32
Dorsal Striatum (L)	DS.L	-23.91	3.86	4.00

Figure S1. Sensation seeking scores distribution.